JOURNAL OF MATERIALS SCIENCE 20 (1985) 4259–4297

Review
Preparation of glass by sintering

E. M. RABINOVICH
AT & T Bell Laboratories, Murray Hill, New Jersey 07974, USA

Preparation of glass articles by sintering of glass and amorphous powders is considered. The classification of sintering processes includes: (a) sintering of premelted and pulverized glasses; (b) sintering of premelted chemically treated glasses; (c) sintering without melting; (d) sintering with melting. The most interesting class of processes is sintering without, or simultaneously with, melting and it includes preparation of preforms for optical fibres and the sol–gel route for glass preparation. This last route is reviewed in detail. Two main versions are considered: preparation of gels by hydrolysis and polymerization of alkoxides, and sintering of amorphous colloidal powder compacts. The sol–gel processes represent an embryo of a new technology for the production of high-melting glasses (including quartz glass) at relatively low temperatures.

1. Introduction and classification

Preparation of glass by sintering rather than melting allows the reduction of technological temperatures and the formation of complex shapes by the methods of ceramic technology. The practical melting temperature of a glass is significantly higher than the thermodynamic melting point (the liquidus temperature) of a crystal mixture of the same composition, because high viscosity at the liquidus temperature slows the dissolution of particles and arrests refining of glass. Some examples [1, 2] are given in Table I. Sintering of pulverized glass or amorphous powders provides a possible alternative to melting at high temperatures. Because both melting and sintering involve consolidation by viscous flow (this process will be considered later), it is useful to begin with definitions. We will define the consolidation of amorphous powders to a bulk glass as pure sintering if the process takes place fully below the liquidus temperature for that composition. If the consolidation takes place above the liquidus it will be usually referred to as melting, but with a few reservations discussed below.

It is neccessary to explain why we attribute such a significance to the liquidus temperature, since it is the equilibrium temperature for melting of crystal phases and does not represent any specific change or transition for a glass. Really, there is no difference in mechanism and only a slight difference in kinetics if, for example, an amorphous silica powder is sintered either at 1715 or 1730° C (the liquidus is at 1723° C, [2]). However: (a) below the liquidus only amorphous starting particles may be sintered to a bulk glass, while above the liquidus crystalline starting particles will melt before or simultaneously with the consolidation; (b) below the liquidus, crystallization may occur in the course of sintering, thus arresting it; above the liquidus there is

TABLE I Comparison of the liquidus and practical melting temperature for several glasses [1, 2]

Type of glass	Liquidus temperature (° C)	Technological melting temperature (° C)
Flat and bottle glasses	950 to 1050	~ 1500
Borosilicate laboratory ware (Pyrex)	< 1200	~ 1600
Fused silica	1723	1800 to 2000

0022–2461/85 $03.00 + .12

no danger of crystallization and the consolidation may be improved by an increase in temperature or time.

In addition to this, the quite definite liquidus temperature is a convenient mental point for separation between sintering and melting. It is more difficult to divide just-above-liquidus melting and far-above-liquidus melting. Just above liquidus the viscosity is usually high, and this is the reason why conventional production of glass from the mixture of starting materials (batch) cannot be completed at these temperatures in a reasonable time. Far above liquidus these processes can be carried out more readily.

A significant technological difference between sintering and melting is that shapes for sintering are formed before or during sintering, while in case of melting, formation is usually the final step of the process. However, this difference does not have any relation to the liquidus temperature, and the cold-formed shapes may sometimes be retained at high viscosity of just-above-liquidus melting. Therefore we may refer to this kind of melting as a mixture of sintering and melting.

Sintering as a method of glass preparation is not a new concept. Really it is as old as glass technology itself. More that 2500 years ago, reliefs and ornaments on the walls of the palace of the Babylonian king Nebuchadnezzar II (604 to 562 BC) were coated by a glaze (e.g. [3]) which is essentially a sintered glass. However, development of soot processes for the preparation of optical fibre preforms [4–6] and of sol–gel processes [7–9] could make sintering a common occurrence in the preparation of glass. Fig. 1 shows our attempt to systematize the processes of glass preparation by sintering. The scheme includes two divisions of premelted and subsequently sintered glasses, and two divisions of sintering before or simultaneously with melting. Below we give a review of every type of sintering. This is neither a comprehensive, nor a uniform review. We have not intended to give a detailed review of glazes or enamels or of the ample literature on Vycor; these and some other glasses are considered briefly or merely mentioned for the completeness of our systematization. A relatively new approach to the preparation of bulk transparent glasses without melting is more interesting and will be reviewed in more detail.

2. Theory and general considerations

The theory of glass sintering is based on theory of viscous flow of Frenkel [10] which has been developed in the works of Mackenzie and Shuttleworth [11], Kuczynski and Zaplatynskyj [12, 13], Cutler and Henricksen [14–16], Kingery and Berg [17] and others; a review of this theory was presented in a monograph [18]. General consideration of the sintering physics was given by Geguzin [19]. A recent review of the liquid phase sintering was presented by Petzow *et al.* [20]. In crystalline ceramic materials and metals other mechanisms of sintering can occur [18, 19]

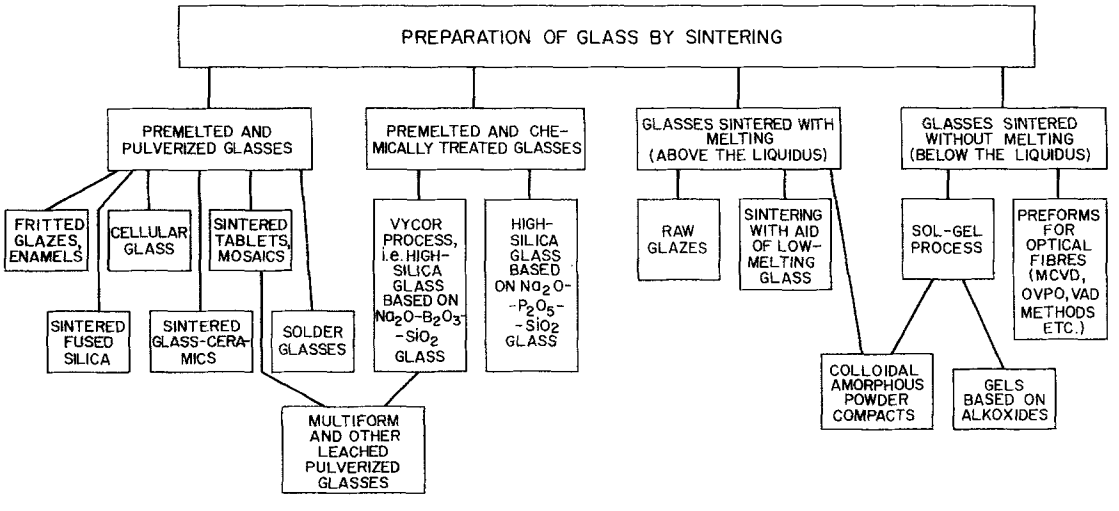

Figure 1 Classification of sintering processes for glass preparation.

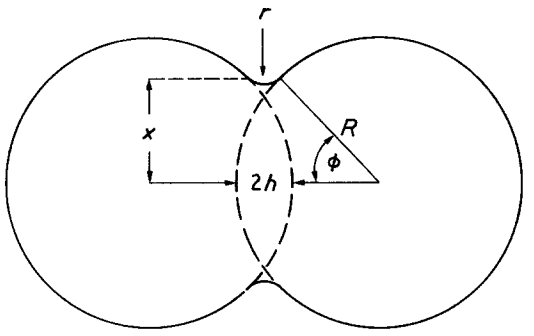

Figure 2 Two spherical particles at initial stages of sintering (after Geguzin [19]).

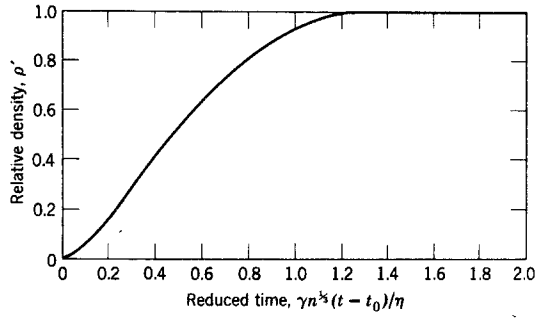

Figure 3 Relative density of a compact of a viscous material as a function of the reduced time (after Mackenzie and Shuttleworth [11]).

such as solid-state sintering, or sintering through vapour transport. However, for sintering of glassy particles the mechanism of viscous flow is more significant and only this mechanism is considered here. Competition between the viscous flow and gas transport from glass layers under sintering is considered in Section 6.2.2.

Two spherical particles in contact (Fig. 2) have a small negative radius of curvature r compared with the radius of the underformed spheres [18, 19]. This causes a transport of material into the pore region by viscous flow. The rate of initial neck growth is determined [10, 18, 19] as

$$\frac{x}{R} = \left(\frac{3\gamma}{2\eta r}\right)^{1/2} t^{1/2} \tag{1}$$

where γ is a surface tension, η is viscosity, t is time; x and R are defined by Fig. 2. The shrinkage is determined as

$$\frac{\Delta V}{V_0} = \frac{3\Delta L}{L_0} = \frac{9\gamma}{4\eta R} t \tag{2}$$

The time for full coalescence of the particles with original radius R_0 is of the order of magnitude of

$$\tau \approx \frac{h}{\gamma} R_0 \tag{3}$$

if $x \approx R_0$. Here $h = R(1 - \cos\phi)$ (see Fig. 2) [19].

A large body with closed pores is formed with time and its rate of densification can be determined [11] as

$$\frac{\gamma n^{1/3}}{\eta}(t - t_0) = \frac{2}{3}\left(\frac{3}{4\pi}\right)^{1/3} \int_0^{\varrho} \frac{\mathrm{d}\varrho}{(1 - \varrho')^{2/3}\varrho'^{1/3}}, \tag{4}$$

where n is the number of pores per unit volume of solid material, ϱ' is the relative density and t_0 is an arbitrarily chosen constant corresponding to $\varrho' = 0$. The value $\gamma n^{1/3}(t - t_0)/\eta$ is called "the reduced time". Fig. 3 shows the dependence of relative density on the reduced time at constant temperature [11, 18].

Experimental data for a soda-lime–silica glass [11] are given in Fig. 4. While solid lines represent treatment of these data according to Equation 3, the dashed curves for the initial stages of sintering were calculated from Equation 2; both types of curve show good agreement.

Kuczynski and Zaplatynskyi [13] examined Frenkel's theory by studying the change in diameter of Pyrex capillaries for various heat treatments. They confirmed the theory and stated that viscous flow is a main mechanism for determining the rate of closure of pores.

Scherer [21–23] considered sintering of bodies with open porosity. The model chosen by him [21] consists of a cubic array formed by intersecting cylinders of radius a and length l; the cylinders represent the strings of spherical particles (Fig. 5). This is, in some degree, a

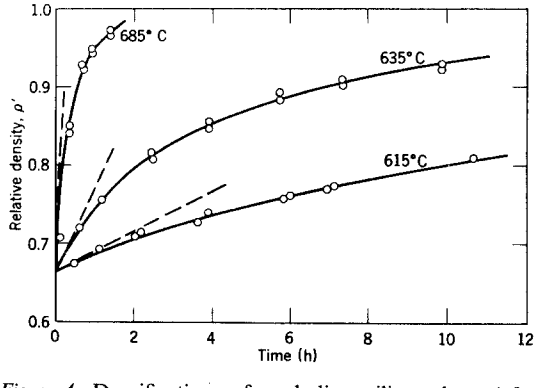

Figure 4 Densification of soda-lime–silica glass (after Kingery *et al.* [18]).

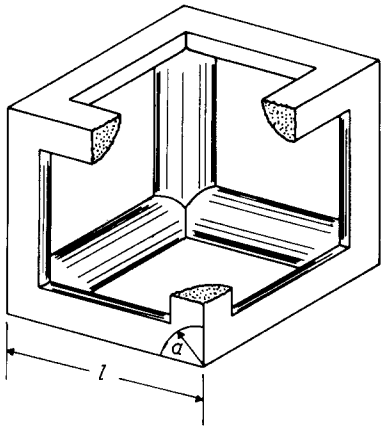

Figure 5 Initial cubic array of sintered spherical particles (after Scherer [21]).

simplified structure because it does not take into account that every cylinder is not a solid body but is initially a chain of spheres in contact. The surface areas calculated from this model were therefore lower than the measured values of ~35%. Scherer determined the limit of existence of the porous structure described by this model by a value for $x = a/l = 1/2$ when the relative density $\varrho' = 3\pi/4 - \sqrt{2} = 0.942$. At higher densities closed porosity appears and the analysis of Mackenzie and Shuttleworth [11] can be applied. Combining both approaches, Scherer [21] plotted a curve of the relative density ϱ/ϱ_s against reduced time defined as $(\gamma/\eta l_0)(\varrho_s/\varrho_0)^{1/3}(t - t_0)$, where ϱ_s is the theoretical density, ϱ_0 is the initial density, l_0 is the initial value of l, and t_0 is the fictitious time for $x = 0$; this curve is given as a solid line in Fig. 6. Experimental data can be fitted to the theoretical curve by plotting real times corresponding to the given density against reduced times from the theoretical curve. The experimental data obtained by Scherer and Bachman [22] for an SiO_2 soot preform fit the theoretical curve very well (Fig. 6). The theory was used to calculate the viscosity of different glasses from sintering data; the results were in good agreement with direct viscosity measurements.

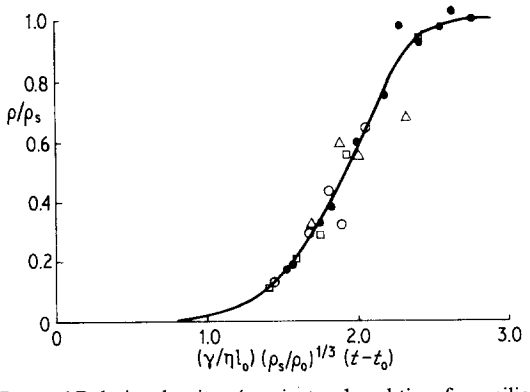

Figure 6 Relative density ϱ' against reduced time for a silica soot preform fired in air (after Scherer and Bachmann [22]); (○) 1115° C, (●) 1185° C, (□) 1236° C, (△) 1327° C.

Scherer also considered sintering of inhomogeneous glasses with wide distributions of pore sizes [21] and with variations in viscosity [24].

An interesting experimental study of sintering of monodispersed amorphous silica particles was published by Shimohira *et al.* [25]. Monodispersed particles (0.2 to 0.6 μm) with a very low standard deviation in the diameter were prepared by hydrolysis of ethylsilicate in the presence of ammonia. Mixing of several batches of the suspensions (each containing differently sized particles) produced a distribution of particle sizes. If the suspension was allowed to settle slowly and then was carefully dried in air, face centred cubic close packing of the spheres was found by electron micrography. If this mass was ground in an agate mortar and then pressed, compacts with random arrangements were formed. The specimens were fired at pre-determined temperatures for 24 h in air.

Random array of uniform-sized particles (0.3 μm) fired at 800° C showed two peaks of pore size distribution at about 25 and 70 nm (Fig. 7a). Packing density of the compact increased at this firing from 0.50 to 0.56. Firing at higher temperatures resulted in further densification, lowering of the peaks and their shift to a smaller position. Random arrays of non-uniform spheres demonstrated only one peak (Fig. 7b), at 42 nm for 800° C. In this case an increase in temperature (from 600 to 800° C) resulted in shift of the peak to a higher position. Scanning electron micrography showed a local pore growth attributed to induced stress caused by the differences in particle sizes. As seen from Equation 1 the rate of the neck growth depends only on the curvature of the neck (assuming γ and η are constant). It is possible to assume that two spheres of different sizes supply about an equal amount of the material to the neck; therefore the decrease of particle size will be inversely proportional to its original size. This causes a void to grow on the opposite side of the smaller sphere. Large particles form the three-dimensional network, and they are linked to

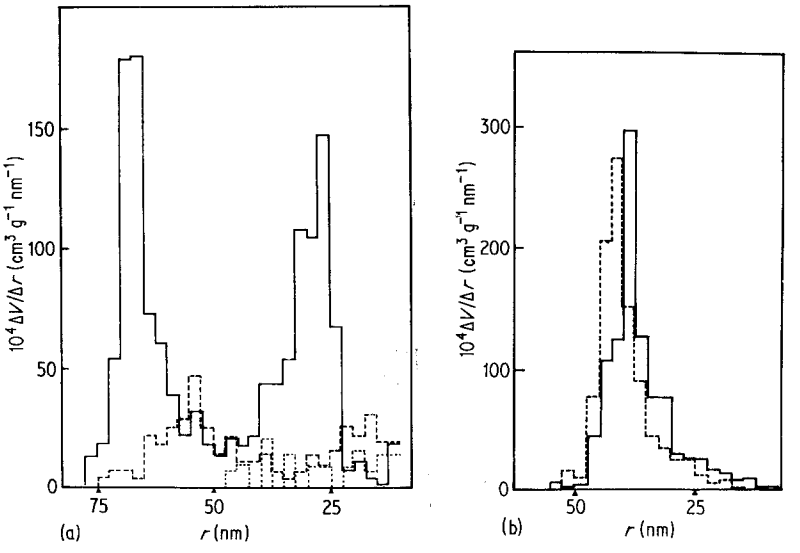

Figure 7 Pore size distribution for random arrangements of (a) monodispersed silica spheres (0.3 μm), and (b) non-uniform sized spheres, both after the latter heat treatment for 24 h (after Shimohira *et al.* [25]).

each other with necks formed at contact points; therefore, pore growth most probably occurs at voids surrounded by smaller particles. This is an explanation of pore growth in an aggregate of non-uniform spheres [25].

An ordered arrangement of uniform spheres is shown in Fig. 8. This structure, from geometrical considerations, should exhibit two kinds of voids, one of which is smaller tetrahedral voids and the other is larger octahedral voids. This kind of distribution was observed experimentally. Rearrangement of the particles is difficult in this situation, and all voids will shrink without changing their relative positions. Hence, at firing, larger voids tend to shrink before smaller ones and this results in a shift of pore sizes to smaller values, similar to the random array of uniform spheres. Therefore, uniformity in particle size is more favourable for sintering.

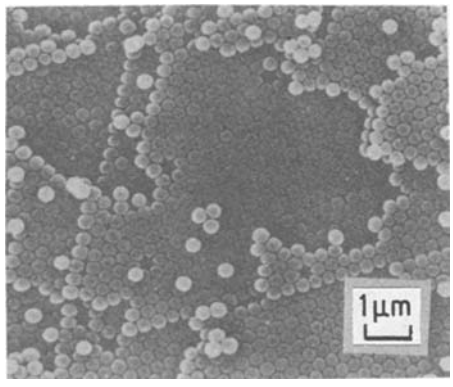

Figure 8 Face-centred cubic array of uniform sized particles, after heat treatment at 800° C for 24 h (after Shimohira *et al.* [25]).

Shimohira *et al.* [25] concluded that rearrangement of the particles is a very important first step of the sintering process.

3. Sintering of premelted and pulverized glasses and glass–ceramics

We include in this group all kinds of consolidation of previously melted and pulverized glasses.

3.1. Fritted glazes and enamels

Glazes [26] and enamels [27] are melted in pot or tank furnaces and cooled by pouring into water or with the help of water-cooled rollers. They undergo wet milling; colour and opacifying agents are introduced either during the milling, or they may be put into the original batch before the melting. After application to a ceramic or metal surface, glazes and enamels are fired. The firing temperature is mainly determined by viscosity and may be either below or above the liquidus temperature. Some glazes may crystallize in the course of their sintering, which makes them similar to the crystallized solder glasses considered below. Various kinds of glassy coatings are described by Appen [28] and by other workers [29].

3.2. Cellular (foam) glass

This glass [1, 30] is produced, as a rule, from a pulverized glass heated together with a gas former such as fine carbon, magnesium and calcium carbonates and others substances. Sintering and foaming result in formation of a light material

(bulk densiy 0.14 to 0.6 g cm^{-3}). containing nearly 90% voids, which is an excellent non-combustible thermal insulator (thermal conductivity is 0.06 to 0.17 J sec^{-1} m^{-1} K^{-1} at 20° C). It is used for cold and hot insulation up to 400 to 500° C; however the high-silica cellular glass "penosil" [30] may endure temperatures as high as 1050° C. Some foam materials may be produced directly from raw materials such as low-melting clays by way of their simultaneous sintering, melting and foaming [30].

3.3. Sintered glassware

Glass articles of complicated shape can sometimes be more easily moulded from powder by ceramic methods (pressing, slip casting etc.) than by methods of glass technology [1, 31–34]. The articles, fired at temperatures above softening, have about the same properties as a parent glass, however they are usually not transparent due to retained porosity [1] and have lower mechanical strength. Depending on the sintering temperature, the articles may contain open porosity or they may be vacuum-tight [34]. Porous glasses include fritted filters [1, 34], while vacuum-tight articles, sintered at higher temperatures, include smarts, mosaics, and tablets for electronics. Some articles may be produced by mixing powders of different glasses, which allows alteration of the properties of the original glasses. Table II, taken from the book by Rous [34], shows how mixing of two glasses (used in electronics) permits the changing of properties.

Properties of sintered glasses, such as dielectric permittivity, dielectric loss (tan δ), electric and heat conductivities, are strongly dependent on the porosity which depends on the particle size. Fig. 9, taken from Volf's book [33], shows the dependence of the closed porosity on the particle size for several glasses. As the figure shows, the smaller the particles the higher the porosity. This somewhat paradoxical result can probably be explained by dispersion around the average size. As was shown by Shimohira *et al.* [25] (see Section 2), pores can grow around small particles in an array of non-uniformly sized grains forming larger voids. Increased porosity results in significant decrease in the electric conductivity; the dielectric permittivity and tan δ are also reduced [34]. The porosity has the most pronounced effect on the heat conductivity since a reduction in the bulk density of only 15% corresponds to a 25% reduction in the heat conductivity (this effect occurs in cellular glasses). Sintered glass crystallizes more rapidly than the same glass in a bulk form due to the higher surface area of the former [34] (see also Section 3.5).

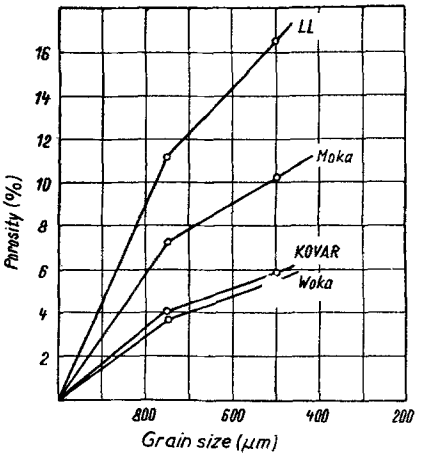

Figure 9 Porosity as a function of powder particle size for several glasses (after Volf [33]).

Seals of metal leads with sintered glass are shown in Fig. 10 [34]. Glass cullet is pulverized in ball mills in methanol with additions of

TABLE II Properties of mixed sintered glasses, after Rous [34]

Composition	Sintering temperature (° C)	Linear shrinkage (%)	Linear coefficient of thermal expansion at 20 to 300° C (° C)$^{-1}$ × 10^7	T_g (° C)	T_k - 100 (° C)†	Tan δ at 10^6 Hz and 20° C × 10^4
I*	660	18	95.1	450	307	20
75% I + 25% II	720	20.8	85.2	475	287	31
50% I + 50% II	790	21.3	74.0	526	281	38
25% I + 75% II	800	20.3	63.9	570	253	50
II‡	800	17.3	58.1	595	203	80

*Glass containing BaO and Li_2O.
†Temperature corresponding to 100 Ω cm electrical resistivity.
‡Glass KS50.

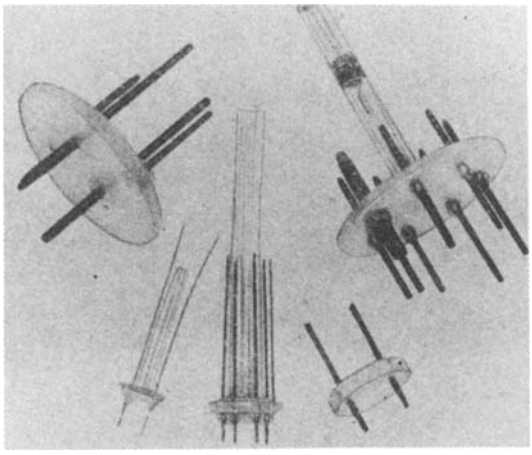

Figure 10 Articles prepared from sintered glasses. Leads are made from molybdenum or lead (after Rous [34]).

NH_4OH or an aqueous solution of $LiNO_3$. For proper placing of metal leads and subsequent sintering, graphite moulds are used.

The lower heat conductivity of sintered glass may require the use of a hotter flame for sealing a detail to a glass bulb. To overcome this disadvantage, a ring of a bulk glass can be put into the mould around the sintered glass so that the ring will serve as an intermediate between the sintered glass and the bulb [34].

Small sintered tablets with holes for metal leads are pressed from a glass powder with particles sized below 300 μm. Paraffin, nitrocellulose solutions, or various resins are used as admixtures during pressing. The tablets are sintered in conveyer kilns at 600 to 700° C. The metal used is usually kovar, requiring that the linear coefficient of thermal expansion of the glass should be near $50 \times 10^{-7} \circ C^{-1}$. The sealing of previously sintered tablets with kovar which has been etched and fired in hydrogen is conducted in a reducing atmosphere (e.g. in a 3 : 1 mixture of N_2 and H_2) with traces of oxygen or water vapour. (These traces should provide a thin layer of metal oxide on kovar.) Alternatively, the metal can be previously oxidized, and then sintering with glass can be done in a neutral atmosphere. Cobalt, chromium or nickel oxides mixed with the glass powder enhance adhesions of glass to metal.

Rous [34] stated that sintered glass has higher themal endurance compared with its bulk counterpart and can tolerate higher differences in thermal expansion when sealed with metals. In contrast with this, Volf [33] indicates that the thermal endurance is mainly a function of mechanical strength, thermal expansion and modulus of elasticity. While the last two parameters are the same for both bulk and sintered glass, the strength is lower for the sintered glass, and therefore its thermal endurance should be lower. The change in the heat conductivity of sintered glass compared with the bulk glass makes the problem of the thermal endurance even more complicated and dependent on the kind of thermal shock. Taking into account the lower strength of the sintered glass, we also cannot understand why a higher level of thermal expansion coefficient difference (i.e. higher stress) [34] can be tolerated with sintered glass.

The described method is sometimes referred to as a "Multiform" method [33, 35], although this designation was originally used only for products made of fused silica of Vycor powder (see Section 4).

Sintering allows the preparation of electroconductive glass–metal composites [34] which can be sealed with other glasses. Sintered fused silica powder containing 10% molybdenum can be used as the current conductor which operates through sintered chain-like molybdenum grains. Thermal expansion of this composite is between that of fused silica and that of tungsten, so it is used as a transition glass for joining fused silica with tungsten. However, the thermal shock resistance of such joints is rather low.

Ground, formed and sintered Pyrex glass has been used for the preparation of funnels, crucibles, gas filters and other kinds of chemical ware [36].

3.4. Sintered fused silica (quartz ceramics)

Fused silica is one of the most valuable glasses: it has a very low thermal expansion, and therefore high thermal shock stability, good dielectric properties, and high softening temperature. However the very high viscosity of molten silica requires high production temperatures (1800 to 2000° C), and manufacture of complex shapes is very difficult. Sintered fused silica (often called "quartz ceramics" although it does not seem to be a very fortunate term) is a material prepared by pulverizing fused silica cullet, moulding by methods of ceramic technology, and sintering. In this way many complex shapes can be prepared.

The process was probably first developed by Skaupy and Weissenberg, [37, 38], although they formed articles from quartz sand rather than fused silica particles; the articles were sintered–melted at 1650 to 1680° C. In the last 20 years sintered fused silica has been under intensive study in several countries [39–50]. Extensive reviews on quartz ceramics have been published by Russian workers [42, 46].

The raw material for sintered fused silica is finely milled powders of waste silica glass [42, 50]. The articles may be formed by different methods, such as hot pressing [39], slip casting [40, 42, 43, 50], spraying and thermoplastic technology [48]. The firing temperature is usually around 1300° C, and this temperature coincides with the crystallization temperatures of fused silica. Crystallization is a highly undersirable phenomenon because its product, cristobalite, has a thermal expansion greatly different from that of fused silica and undergoes a phase transformation with a sharp change of volume at 230° C. Therefore formation of cristobalite in amounts more than 5% results in mechanical destruction of the product. In addition, this crystallization arrests sintering. Fortunately, the rate of crystallization of pure fused silica is low but it strongly depends on impurities (see compilation of these data by Mazurin *et al.* [51]): at 1300° C in air it ranges from 0.01 to 0.1 $\mu m\,min^{-1}$ and in bulk glass there is no crystallization in times as long as 60 h [51]. Even traces of alkali and alkali earth ions drastically increase the rate of crystal lization, as well as crystalline impurities from grinding media; high surface area of the powder also promotes crystallization. Therefore high purity of a starting glassy material is very important: it should contain not less than 99.6% SiO_2 [41] and be free from crystalline admixtures.

Some impurities inhibit crystallization. Primarily, for example, glass formers such as B_2O_3. Small amounts of Al^{3+} ions enhance crystallization but larger amounts inhibit it. However the amount of Al^{3+} necessary for the inhibition is not quite well established and probably depends on other impurities. Budnikov and Pivinskii [42] determined this amount as low as 0.05 wt % Al_2O_3, but they cited data by Kainarskii and Degtyareva who had established that the presence of less than 1.5% Al_2O_3 enhances crystallization. A study of the sintering and crystallization of fused silica was published by Taylor *et al.* [45].

Properties of the sintered material are strongly dependent on processing conditions, which were reviewed in detail by Budnikov and Pivinskii [42]. In the case of slip casting, the higher the density of the original slip the higher is the density of the resulting castings [43]. A higher density was achieved by a two-stage process when a quartz glass was dry-milled and then blended and additionally milled with water. It was shown that a coarse powder (particle size $\leqslant 60\,\mu m$) showed greater thixotropy than a fine powder (particle size $\leqslant 20\,\mu m$); the coarse powder produced material with lower strength and density. Pivinskii and Gorobetz [43] were able to prepare a slip containing as high as 70 to 75 vol % solids which was cast in plaster moulds and gave castings with a bulk density of 1.92 to 2.03 $g\,cm^{-3}$, porosity of 8.5 to 13%, and modulus of rupture of 3 to 7.5 MPa. The relatively high strength of the unfired material was explained by the presence of silicic acid with outstanding bonding properties. Sintering resulted in 2.5 to 9% shrinkage and produced bodies with an average modulus of rupture of 73 MPa, which is almost as high as the values for bulk glasses.

Komarova [50] noted that castings with coarse particles more readily crystallize than castings with fine particles. This seems strange, because crystallization usually begins from the surface and should be greater in the case of a higher surface area. This result can probably be explained by more rapid sintering of fine powders with annihilation of the significant part of the surface before the onset of crystallization. Sintering at 1200 to 1300° C resulted in the formation of not only cristobalite but quartz as well, and the total amount of crystal phase in one of the specimens was as high as 28 wt %. In spite of this, its strength (modulus of rupture 40 MPa) was not lower than for a purely amorphous specimen. This rather high strength seems to be unexpected in view of the tendency of high-cristobalite materials to crack.

Fleming [40] used colloidal silica as a binder and dispersant for the wet grinding of coarse silica to form a slip with 95% of particles less than 50 μm. He prepared hollow castings about 50 kg in weight by conventional castings techniques; the modified method allowed fabrication of parts weighing more than 450 kg.

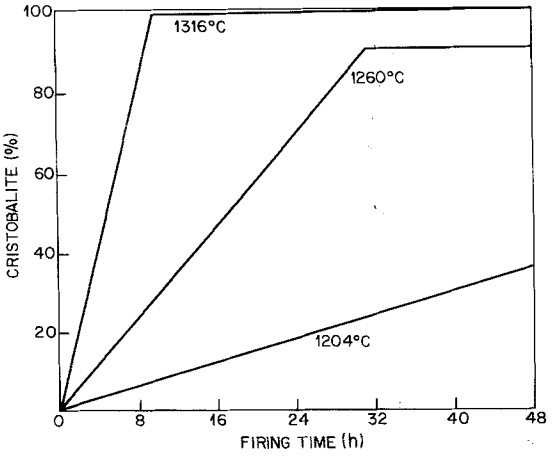

Figure 11 Crystallization of slip-cast fused silica (after Fleming, [40]); Figs. 11 and 12 have been redrawn to adjust them to the metric system.

Figs. 11 and 12 show the dependence of the amount of cristobalite and the modulus of rupture on the firing temperature and time [40]. As seen from comparison of these figures, the highest strength (40 to 45 MPa) was shown by specimens containing less than 5% cristobalite. No quartz formation was described by Fleming [40]. The tensile strength of the silica was of the same order of magnitude as the modulus of rupture and increased with temperature. The open porosity of the slip-cast fused silica decreased to 7% during the 4 h firing at 1260° C.

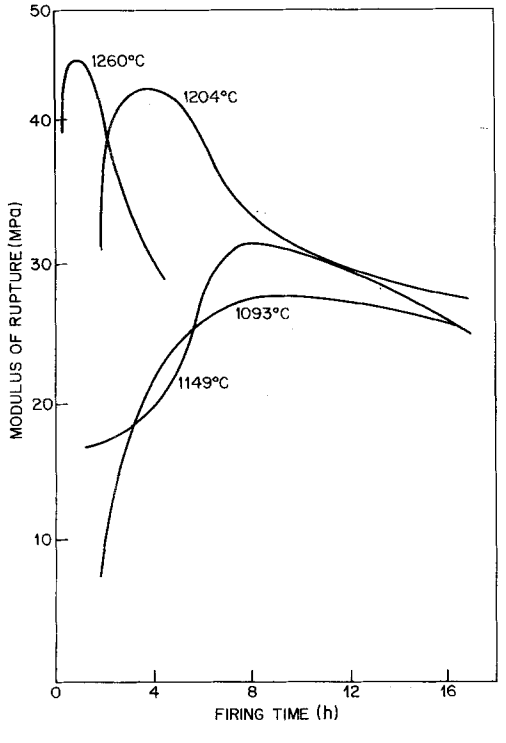

Figure 12 Room-temperature modulus of rupture of slip-cast fused silica as a function of time at different firing temperatures (after Fleming [40]) (see note to Fig. 11).

Different binders have been used for preparation of slip-cast fused silica, such as urea-formaldehyde resin (0.2%) or ethyl silicates [42]. Savitskas and Matusevich [49] described slip casting of a mixture of coarse and fine particles bound with hydrolysed ethyl silicate in the presence of small admixtures of HF. The castings, aided by vibration using a frequency of 60 Hz, were dried at room temperature at 60 to 120° C and fired at 1250° C for 2 h. The compression strength of the resulting material was as high as 150 MPa; the density was 1.90 g cm^{-3} and open porosity 12.4 to 15.3%.

Methods other than slip casting have been used for the preparation of quartz ceramics. Vasilos [39] described hot pressing which permitted consolidation at temperatures as low as 1150 to 1200° C. He found that for this method the effect of particle size on densification within the range 5 to 300 μm was small.

In the case of a very dense starting body (12 to 15% porosity), a quartz glass–ceramic with zero apparent porosity can be prepared [42].

Hot casting with paraffin was also used [42, 48] but the density of the articles was lower than in the case of slip casting [42]. The semi-dry (cold) pressing at 80 to 120 MPa resulted in a product with high apparent porosity (near 18% after firing). The bulk density of the articles after pressing and firing increased with increase in pressure [42].

The atmosphere of sintering has an effect on densification. Tomilov *et al.* [47] found that the shrinkage increases with the humidity of air or nitrogen. They showed a decrease in shrinkage upon sintering in vacuum compared with sintering in air; this result contradicts the results of other researchers. The atmosphere also affects the rate of crystallization. Quartz glass has a higher rate of crystallization in oxygen and in water vapours than in dry nitrogen [42].

Gannon *et al.* [52] studied the dependence on porosity of the mechanical, thermal and dielectric properties of sintered fused silica prepared by different methods. They showed that the dielectric permittivity is dependent on porosity alone and not on fabrication method. It increases from 1.0 at about 13% of the theoretical

density up to 3.7 at 100%. Other properties depend on the method of preparation as well. The bulk density varies with the variation in coarse and fine fractions in an original powder. The thermal conductivity increases with increase in the bulk density, but a large discontinuity exists between all slip-cast materials, very dense hot-pressed silica (95% density, 1% cobalt admixed) and 100% dense transparent (melted) fused silica which exhibits the highest conductivity. The elastic modulus continuously increases with increase in bulk density. In general, the compressive strength also increases with the bulk density, but also depends on the fabrication mode.

Fleming [53] described the disappearance of cristobalite in slip-cast fused silica as a result of irradiation. The original samples were fired at 1370° C for 48 h to ensure extensive crystallization. They contained from 21 to 88% cristobalite. After irradiation in a reactor for 340 MW days the amount of cristobalite was as low as 3 to 8%. This irradiation did not have a noticeable effect on mechanical strength.

Quartz ceramics have found rather wide applications. They can be used for production of free-standing insulators in high-temperature nuclear reactors or for radomes, nose cones and rocket nozzles [53]. For radome application, slip-cast fused silica shows excellent thermal shock resistance, light weight, ease of fabrication at low cost, but poor rain erosion resistance [54]; it can be used for rockets with speed Mach 4 to 5.

3.5. Sintered glass–ceramics

The basic technology of glass–ceramics consists of preparation of monolithic glass articles by the usual means of glass technology and their subsequent crystallization [55, 56]. However this technology requires heavy investment and can be justified only for large volume production. On the other hand, production of glass–ceramics by sintering of glass powders may be done using the ordinary equipment of a ceramic factory and is especially suitable for the manufacture of small quantities of articles with complicated shapes. This technology was developed in the USA [57], the USSR [58, 59], Sweden [60] and Israel [61].

The process involves the following steps: (a) melting of glass and its quenching; (b) pulverizing; (c) formation by means of ceramic technology (slip casting, pressing, extrusion etc.); (d) firing for consolidation and crystallization.

There is a significant difference between glass compositions suitable for conversion to glass–ceramics by methods of conventional technology and compositions intended for sintering [61]. The conventional technology is based on glasses with heterogeneous volume crystallization. The crystallization takes place at high viscosities, preventing significant deformation of glass articles. If such a glass is finely ground and compacted again, every particle will crystallize separately, resulting in an infinite increase in viscosity. Therefore good sintering and high strength of sintered bodies will be excluded.

Rabinovich [61] showed that glasses with surface crystallization are more suitable for the formation of glass–ceramics by sintering. In this case sintering occurs simultaneously with crystallization. In spite of the surface crystallization, uniform volume crystallization is provided by the small size of the separate particles. In this way practically any glass can be transformed into a glass–ceramic. If crystallization is too slow (as in the case of an ordinary plate glass), "seeding" by small amounts (0.1 to 1%) of the same glass in a pre-crystallized state may accelerate and control crystallization and deformation [61].

About 40 glasses based on the composition of cordierite $2MgO \cdot 2Al_2O_3 \cdot 5SiO_2$ were studied by Rabinovich [61]. Some of them had TiO_2 as a nucleating agent; all of these glasses crystallized prematurely and showed poor sintering. Fig. 13 shows the compressive strength of pellets of

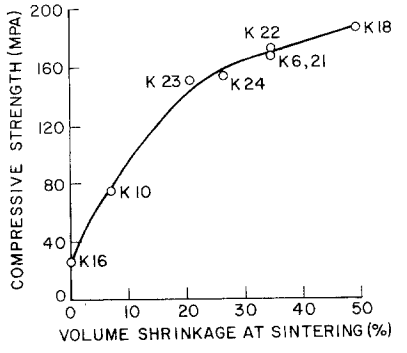

Figure 13 Average compressive strength of pressed powder pellets sintered to 1200° C for 2 h as a function of average shrinkage after sintering. Cordierite compositions with TiO_2 (K10, K16, K23), with P_2O_5 (K6, K18, K24), and without any admixtures (K21, K22) (after Rabinovich [61]).

different tested glasses as a function of the shrinkage. Glass K18 containing no TiO_2 but with 4.5 wt% P_2O_5 in its composition showed the highest shrinkage, crystallization with nearly 80% cordierite in the crystal phase, and an average modulus of rupture of 150 MPa after firing with soaking at 1100° C. It was shown that cordierite in the pulverized glass forms significantly more rapidly than in the same glass in a monolithic state.

Giess *et al.* [62] also chose the cordierite composition with only glass-formers (B_2O_3 and P_2O_5) added. They studied the sintering process of pressed pellets and found pronounced anisotropy of shrinkage as a result of the uniaxial pressing. They found that Frenkel's theory gives a good approximation only to the initial stages of sintering. However the authors [62] did not take into account the interference of crystallization in the sintering process, and did not mention crystallization. Probably it did not occur at the selected low sintering temperatures of 800 to 860° C.

As seen from the cited literature [57–61], practically all work in the field of sintered glass–ceramics has been done with compositions in the cordierite region. This is due to the good dielectric properties, low thermal expansion and good thermal shock resistance of cordierite. Cordierite formation in ceramics is limited by the narrow temperature interval of sintering, which is 1300 to 1400° C [63]. Crystallization of cordierite from glass permits significant widening of this temperature interval [59] and sintering–crystallization at much lower temperatures (below 1100° C). The linear coefficient of thermal expansion of the glass–ceramics thus produced is (23 to 33) $\times 10^{-7}\,°C^{-1}$ [61].

Schiller and Wiegmann [64] reported sintered glass–ceramics in the BaO–Al_2O_3–SiO_2 system.

All this relates to glass–ceramic bodies which should be sintered with little or no deformation. Another kind of powdered glass–ceramics is crystallized solder glasses considered in the next section.

3.6. Solder glasses

Solder glasses are widely used in electronics for vacuum-tight joints between glasses, ceramics and metals at relatively low temperatures. In fact, these glasses can be considered as a particular case of fritted glazes. Solder glasses in the PbO–B_2O_3–ZnO system were described by Dale and Stanworth as early as 1949 [65]; extensive reviews of glass solders have been published by Broukal [66], Rabinovich [67] and Takamori [68].

These glasses are usually prepared as powders dispersed in organic binders. The pastes as prepared are applied between the surfaces to be joined, and (after drying) the firing cycle is applied. During firing, spreading and sintering of the powder provides the seal. As in any case of a seal with glass, the matching of thermal expansion of all materials involved is essential for mechanical integrity of the seal. Certainly the proper spreading of the glass solder should occur at temperatures when other materials in the seal are quite rigid.

Solder glasses (sometimes called glass cements and glass–ceramic cements) can be noncrystallizable or crystallizable. Noncrystallizable solders [65, 66, 67] remain glassy after the firing. Naturally, any subsequent heating of the device cannot exceed the softening temperature of the solder which is significantly below the soldering temperature. Fig. 14, taken from Dalton [69], illustrates this statement. Good spreading and sealing can be done at a viscosity of the glass solder of 10^3 to $10^5\,N\,sec\,m^{-2}$; solder 7570 has these viscosities near 500° C when the soldered glass, No. 0080, has viscosity above $10^{12}\,N\,sec\,m^{-2}$, i.e. it is yet quite rigid glass. After the sealing the seal cannot be heated again above near 300° C when the viscosity of the solder is below $10^{12}\,N\,sec\,m^{-2}$, otherwise deformation and separation may occur. This is a disadvantage of this kind of sealing. If, for example, noncrystallizable solders are used for sealing the face and

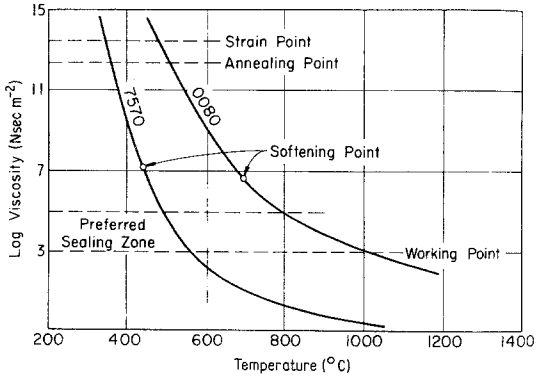

Figure 14 Temperature dependence of viscosity of Corning glass 0080 and solder glass 7570 (after Dalton [69]).

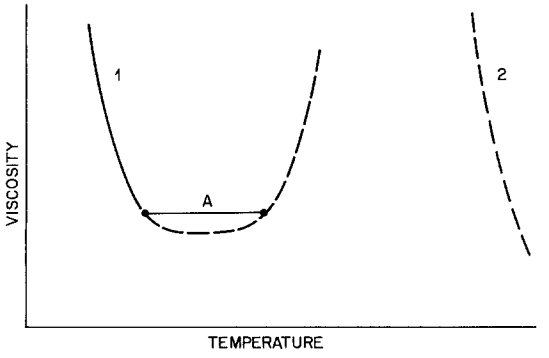

Figure 15 Schematic graph of the temperature dependence of viscosity of a crystallizing solder glass: (1) uncrystallized glass, (A) soldering and crystallization zone, (2) viscosity after melting the crystal phase (after Broukal [66]).

the cone of colour television picture tubes, this property limits the temperature of the tube evacuation and therefore its service life and reliability.

Crystallizable solder glasses have been an excellent reply to this difficulty. They permit soldering in the same way as a noncrystallized solder, but in the course of the spreading and sealing they crystallize and form a glass–ceramic seal. Viscosity increases indefinitely, to decrease again only near the melting temperature of the crystal phase (Fig. 15) [67, 70]. Therefore the seal and the whole device can be reheated not only above the original annealing zone of the solder but even above the soldering temperature.

Crystallizable solder glasses are really a particular case of a sintered glass–ceramic. However, in the case of glass–ceramic articles deformation should be avoided; in the case of the solders it should be encouraged [67]. This indicates a very delicate relationship between sintering and crystallization. Crystallization should not occur too early in order to permit free flow and formation of a good seal. On the other hand, the surface character of crystallization of these glasses [71, 72] requires it to take place before all boundaries between the particles have disappeared. The spreading ability of these glasses is a complicated characteristic determined mainly by viscosity and the crystallization rate, rather than surface energies and the wetting angle as in case of noncrystallizing solder glasses [67, 71]. It was shown [71] that very small admixtures of the same glass in precrystallized form drastically reduce spreading of a solder glass in the $PbO–B_2O_2–ZnO$ system: in fact, addition of as little as 0.01% of the precrystallized glass converts the solder glass into sintered glass–ceramic, capable of crystallization almost without deformation.

Compositions of solder glasses are quite diverse. For sealing at 400 to 500° C glasses in the $PbO–B_2O_3–ZnO$ system are used; the $ZnO–Al_2O_3–SiO_2$ crystallized glasses provide sealing at 700 to 800° C, while for 1000° C sealing, crystallized glasses in the $Li_2O–MgO–Al_2O_3–SiO_2$ system were described [73]. Naturally, the values of the thermal expansion of all these glasses vary between quite wide limits.

4. Sintering of premelted chemically treated glasses

Practically the only example of this glass is a group of Corning glasses with the common trade mark Vycor. We consider this type of glass as one of the most elegant inventions in glass technology of this century, the honour of which belongs to Hood and Nordberg [73]. The scheme of this process, as based on published information [30, 33, 74], is given in Fig. 16. A glass of quite different composition to that of pure silica, taken from the $Na_2O–B_2O_3–SiO_2$ system (with small additions of other components), is melted at 1450 to 1500° C. It is then moulded and heat-treated at 500 to 700° C in order to form a phase-separated interconnected structure. One of the phases is almost pure silica; and the other is an $Na_2O–B_2O_3$ glass which can be leached by

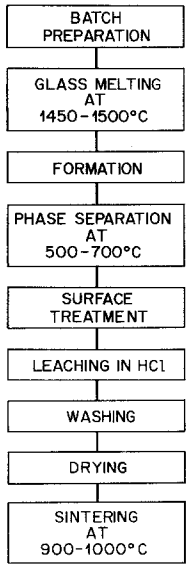

Figure 16 Process chart for the manufacture of Vycor glass.

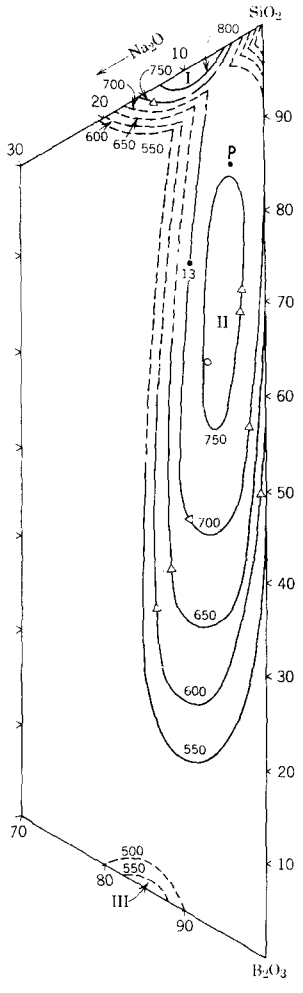

Figure 17 Liquid-liquid immiscibility in the Na_2O–B_2O_3–SiO_2 system (after Haller *et al.* [79]). Point P is added by the author.

hydrochloric acid. After washing and drying a so-called high- silica "thirsty" glass [33] appears, so named because its high surface area is highly hygroscopic. This "thirsty" glass may be used as a virus filter because of its favourable pore size distribution. Sintering at the relatively low temperatures of 900 to 1000° C leads to shrinkage, annihilation of porosity (with conservation of the original shape of an article), and formation of a monolithic transparent glass body containing as much as 96 wt % SiO_2, 3% B_2O_3, 0.4% (R_2O_3 + RO_2) (chiefly Al_2O_3 and ZrO_2),and traces of Na_2O and As_2O_3 [74].

Phase separation is a common occurrence among silicate glasses and melts [75–78]. However, phase separation in the Na_2O–B_2O_3–SiO_2 glass has a rare combination of two features which have made preparation of Vycor possible.

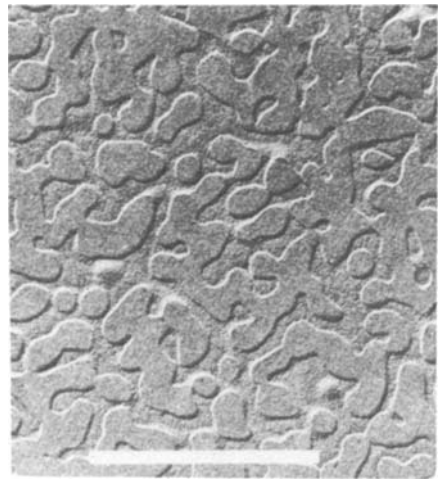

Figure 18 Glass of composition (wt %) 67.4 SiO_2, 25.7 B_2O_3, 6.9 Na_2O after 3 h at 700° C. The silica-rich phase forming an interconnected structure appears to be raised and smooth; the alkali borate-rich phase has a rough surface. White scale bar = 1 μm. (After Elmer *et al.* [80].)

One of them is the formation of a phase which can be selectively leached by an HCl solution, while the other phase remains unreacted. The second feature involves the mutual distribution of the phases which permits the leaching to occur. It is evident that if a soluble phase appears as droplets inside an insoluble matrix, it cannot be leached. Fig. 17 shows a diagram of liquid–liquid immiscibility in the Na_2O–B_2O_3–SiO_2 system [79]. It contains three regions of immiscibility. Region II is a basis for two phase-separated glasses, Vycor (Point 13 on the diagram) and Pyrex (Point P), but they belong to different parts of this region. Pyrex forms B_2O_3-rich drops (about 5 nm in diameter [18]) in an SiO_2-enriched matrix. This increases the chemical durability of the matrix, and hence that of the whole glass. In contrast with this, the interconnected structure (Fig. 18) [80] of the Vycor-precursor glass is open for leaching of a sodium borate constituent. The optimum region of compositions for Vycor was determined [33] to be, in wt %, SiO_2 55 to 70; Na_2O 10 − 0.1 × (SiO_2 − 55); B_2O_3 the balance (30 to 21.5). Small additions of Al_2O_3 (up to 4%) make the glass more stable against devitrification at sintering.

Sintering of the leached porous glass was studied by Elmer [74]. The glass specimens were sintered in dry air (dew point of − 43° C). Fig. 19 shows that although the glass undergoes a steady contraction from room temperature to

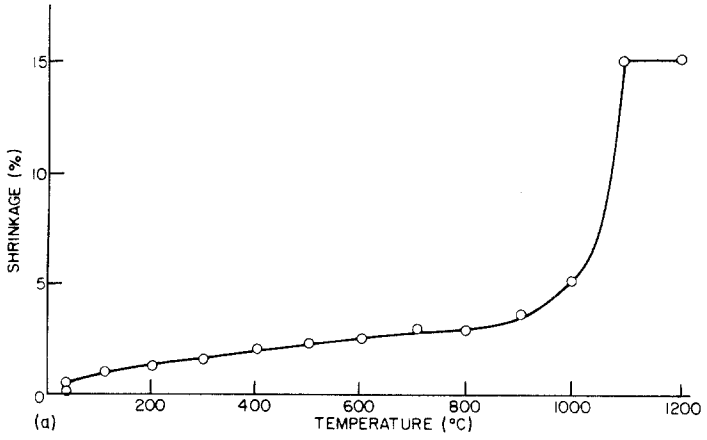

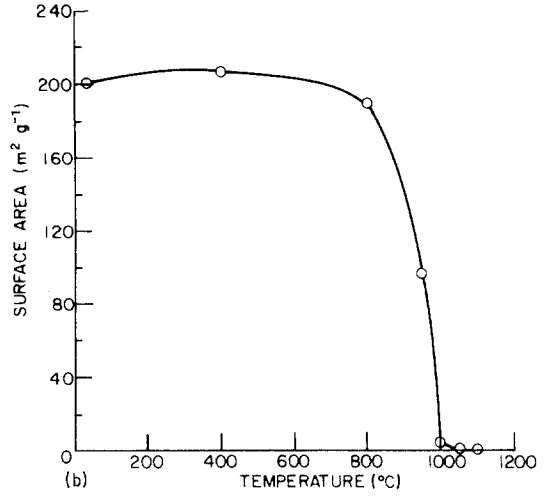

Figure 19 Sintering of wet leached porous glass at a rate of 100° C h^{-1} with soaking for 1 h at temperatures indicated by circles: (a) shrinkage (b) change in the BET surface area (after Elmer [74]).

900° C (Fig. 19a), there is practically no change in the BET surface area up to 900° C (Fig. 19b). Above 900° C rapid sintering takes place, and at 1000° C the porous structure is essentially consolidated into a clear, impervious glass [74].

The properties of Vycor are rather similar to those of fused silica: the linear coefficient of thermal expansion at 20 to 300° C is 8×10^{-7} ° C^{-1}, the maximum working temperature is 800° C (1000° C for fused silica), the refractive index is 1.458 and the density is 2.18 [33]. Tubes, flat glass, crucibles and other shapes can be prepared according to the Vycor technology.

The slowest process in the preparation of Vycor is leaching. Practically this is a very time-consuming process if the wall thickness is more than 3 mm [33]. For this case Greene [35] offered a method of formation of articles from powdered fused silica mixed with dried leach fractions of Vycor. The sintered glass is leached and sintered again. This method originally received the name "Multiform", and it allows the production of thicker articles with properties similar to that of Vycor. Waste of Vycor-precursor glass also may be utilized in this process [34]. It is really an intermediate process between two methods of preparation of glass by sintering (see Fig. 1).

Kitaigorodskii [81] mixed fine powdered fused silica with a borosilicate glass. The partially sintered and leached glass was resintered at 1200° C.

When we consider Vycor as the only example of chemically treated and sintered glass, we are referring to its technological and commercial success. However, apparently a similar type of a phase separation structure suitable for leaching and sintering can be obtained in other systems. Rabinovich *et al.* [82, 83] studied metastable liquid immiscibility in phosphate–silicate systems, and they discovered a wide region of immiscibility in the Na_2O–P_2O_5–SiO_2 system. Several glasses could be leached to form a high-silica skeleton, but only one could be sintered in a bulk glass without crystallization. The composition of a parent glass was $3Na_2O \cdot 7P_2O_5 \cdot 10SiO_2$ (33.75 wt % SiO_2, 55.8% P_2O_5 and 70.95% Na_2O). The resulting glass contained 91 wt % SiO_2, 8.3% P_2O_5 and 0.5% Na_2O. After sintering at 1100° C it had a bulk density of 2.11 g cm^{-3} (92% of the theoretical density) and a linear coefficient of thermal expansion of

$16 \times 10^{-7}\,^{\circ}C^{-1}$. Substitution of SrO for Na_2O resulted in an increased SiO_2 content in the matrix up to 95 wt %, but this glass could not be sintered because of strong crystallization. Probably the introduction of Al_2O_3, as in the case of Vycor compositions, could reduce the tendency of these glasses to crystallization and improve sintering.

Res *et al.* [84, 85] prepared porous glass and glass–ceramic materials on a non-silicate basis. Substitution of $CeO_2 \cdot xNb_2O_5$ (x = 1 to 7) for SiO_2 in the Na_2O–B_2O_3–SiO_2 system resulted in glasses where a sodium borate-rich phase was formed after heat treatment at 650 to 800° C [84]. After melting in a Pt/Rh crucible this phase could be leached in boiling distilled water, forming porous crystalline material with $Ce_2O_3 \cdot 3Nb_2O_5$ (perovskite-type) as a main crystal phase. Melting in alumina crucibles produced almost crystal-free porous glasses. The BET surface area of these materials ranged between 11 and 217 $m^2 g^{-1}$ [84]. Other materials were prepared on the Na_2O–B_2O_3 basis with La_2O_3, Y_2O_3, ZrO_2, ThO_2 and HfO_2. The leached specimens were sintered at 1520° C for 30 min [85]. However, practically none of the properties of these materials have been reported except chemical durability for the last group. It is therefore difficult to judge the practical applicability of these materials.

In principle it is not necessary to have a continuous matrix remaining after phase separation and leaching. If the leached phase forms a matrix, then the leaching will result in the formation of a powdered compact. There is no reason why such a compact cannot be sintered. In fact, similar compacts formed from colloidal gels or by different deposition techniques and described in Section 6 were successfully sintered. However, in the presence of small amounts of Na_2O, which strongly accelerates crystallization of high-silica glasses [86], the rate of crystallization may be dependent on the geometry of the surfaces. Apparently this happened in several cases described by Rabinovich *et al.* [82, 83] where high-silica leached compacts, very similar in their composition to the "thirsty" glasses, could not be sintered without crystallization.

5. Sintering simultaneously with melting

Here we mean sintering at temperatures not very much above the liquidus for articles whose shapes were determined before the heating. We are including here sintering of high-viscosity glass powders and sintering of crystal powders with the help of low-melted glasses; this process is realized in many ceramic processes, but the resulting material is not glass. Some gel-derived glasses considered in Section 6 can be taken to the liquidus temperature to melt crystals formed during sintering. However, the only practical group of materials in this section is raw glazes.

5.1. Raw glazes

Fritting, i.e. preliminary melting and pulverizing of the glazes, may be necessary if a glaze contains water-soluble ingredients such as borax or soluble lead compounds [26]. Melting converts these into silicates insoluble in water and allows the preparation of an aqueous slip. Lead silicates should also be insoluble in gastric juices. If there are no soluble materials in the original batch fritting is not neccessary. In this case wet-mixed raw materials which form a slip can be applied directly to a ceramic body (by dipping or spraying) and fired with the formation of a thin glass layer, transparent or opaque, colourless or coloured. This type of glaze was used in ancient time, e.g., in Nebuchadnezzar's palace, and is still used mainly for sanitary ware and construction materials and tiles.

A batch of raw glaze is a mixture of crystalline raw materials and water, although fritted glaze can also be added. In contrast with a fritted glaze or a solder glass, which can form a coating below the liquidus, a raw glaze should be heated to full melting, homogenization and refining from bubbles. However, because a thin layer of the glaze is easily permeable to gases and because glazes usually have a relatively low viscosity even at the liquidus temperature, significant superheating is not necessary. For more detailed knowledge of raw and fritted glazes the reader is referred to the comprehensive book by Parmellee [26].

6. Glasses sintered without melting

6.1. Sol–gel processes

At the meeting of the Materials Research Society in Albuquerque in February 1984, Uhlmann *et al.* [87] presented a lecture which was entitled "The Ceramist as Chemist – Opportunities for New Materials". This title is

remarkable. In fact, ceramic and glass science always has been a part of chemistry, and ceramists are certainly chemists. However, in the majority of traditional ceramic processes the basic chemical reactions happen at high temperatures, sometimes depriving a ceramist from direct observation and the ability to interfere with an already programmed process. Not rarely, the direct chemical activity of a ceramist is limited to choosing appropriate materials which will react in a furnace.

The emergence of the sol–gel branch of glass and, more widely, the entire ceramic technology has completely changed this situation. It has returned a ceramic scientist to probing tubes, to the mixing of solutions, to pH measurements, and requires knowledge in inorganic, organic, colloidal and physical chemistry. The assortment of chemicals on the laboratory shelf of a ceramist has begun to be similar to that at a typical chemical laboratory. This alone makes the sol–gel route a gift to the scientist beyond industrial applications which, we hope, await this technology.

In 1969 Roy [88], in a short note, drew attention to the possibility of preparing very homogeneous glasses and ceramics by the sol–gel method due to mixing on a molecular level. Dislich [89] was probably the first who prepared glass from a gel.

There are two significantly different kinds of sol–gel technology: (a) hydrolysis and polymerization of alkoxides, and (b) sintering of colloidal gels.

6.1.1. Alkoxide methods

This group of methods has been developed in works by Brinker [8, 9, 90–92], Dislich [8, 9, 89], Klein [8, 9, 93], Sakka [7–9, 94, 95], Yoldas [9, 96–99], Zarzycki [8, 9, 100–103] and others [8, 9]. It was recently reviewed by Sakka [7]; the collection of proceedings of two international workshops on glasses from gels have been published [8, 9], and several other conferences dealt exclusively or in noticeable degree with this problem [104, 105].

Of course, heating at relatively high temperatures to complete glass preparation is involved in this process as well as in traditional ceramic processes. However, a significant novelty of the alkoxide sol–gel methods is the formation of a three-dimensional glass network from solutions at room or slightly elevated temperatures.

6.1.1.1. Gel formation and structure. Metal alkoxides are compounds $M(OR)_n$, where M is a metal and R is an alkyl group [7]; e.g. tetraethyl orthosilicate (TEOS), $Si(OC_2H_5)_4$. The preparation and properties of metal alkoxides are described by Bradley *et al.* [106]. In its most simplified form, the process for TEOS (as an example of alkoxides) can be described by two equations for hydrolysis (Equation 5) and polymerzation (Equations 6 and 6a):

$$Si(OC_2H_5)_4 + 4H_2O = Si(OH)_4 + 4C_2H_5OH \quad (5)$$

and

$$Si(OH)_4 \rightarrow SiO_2 + 2H_2O \quad (6)$$

or

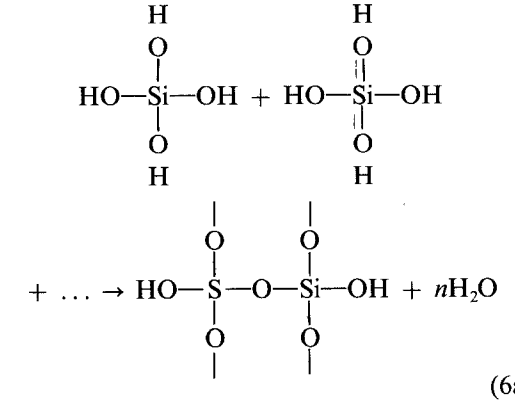

(6a)

The second reaction results, as a rule, in the formation of a gel body. Careful drying will yield, in principle, a monolithic high-porosity body which can be sintered at relatively low temperatures (900 to 1400° C) to produce glass, which otherwise could be done by conventional melting at much higher temperatures (up to 2000° C for fused silica).

In reality, however, the process is much more complex. First, alkoxides and water are immiscible at room temperature and significant additions of an alcohol as a common solvent are necessary. (Recently, Tarasevich [107] reported the mixing of an alkoxide and water and hydrolysis without alcohol, using ultrasound.) Second, both reactions are not completely separated in time, but to a significant degree they take place simultaneously. Relatively slow

hydrolysis of TEOS results in the formation of intermediate chain structures, especially when less than 4 mol H_2O are mixed with 1 mol TEOS [98]. Third, the structure of the product is strongly influenced by either acid or base catalysts and by temperature. Fourth, the drying of a structure with very high surface area (100 to 1000 $m^2 g^{-1}$) and pores with diameter 1 to 7 nm is very difficult, and leads to mechanical breaking of the gel body if special techniques of drying are not applied. Fifth, preparation of multicomponent glasses from a mixture of alkoxides of different metals is complicated by the different rates of hydrolysis of different alkoxides. Sixth, sintering of a high surface area glass body at below the liquidus temperature may be accompanied by its crystallization.

Reaction 6 or 6a is given in a rather simplified form, because it does not take into consideration the different chemical compositions of the silica surface, and this could not be neglected at surface areas as high as 100 to 1000 $m^2 g^{-1}$, depending on the conditions of preparation. The surface chemistry of silica has been extensively reviewed by Iler [108]. The siloxane (SiOSi) surface of silica contains residual valences which react with water at room temperature forming silanol (SiOH) groups. According to the review by Belyakova *et al.* [109], the concentration of the silanol groups on the surface does not depend on the nature of the underlying silica and is equal about $11 \pm 1\,\mu mol\,m^{-2}$, or 6.6 OH groups per nm^2. It is easy to calculate that for silica with a surface area of 800 $m^2 g^{-1}$ every mole of silica will contain as many as 3.2×10^{23} OH groups, such a silica would have the approximate formula $SiO_{1.7}(OH)_{0.6}$; the general expression for high surface area silica is $SiO_{2-n}(OH)_{2n}$. Correspondingly, Reaction 6 should be written

$$Si(OH)_4 \rightarrow SiO_{2-n}(OH)_{2n} + (2 - n)H_2O \qquad (6b)$$

The value of n is a function of the surface area which is strongly dependent on all variables of the process. Krol and van Lierop [110] showed that heat treatment of the gel results in a significant reduction of the amount of (OH) groups per unit area of the surface, even before significant sintering takes place.

The structure of a formed gel and its surface area are strong functions of pH. If an acid is used as a catalyst, and even in the case of subsequent partial neutralization of the acid by NH_4OH up to pH 7.80, random polymer molecules without a distinct surface are formed, as shown by Brinker *et al.* [90]. Yoldas [98] gave a detailed consideration of different polymer configurations of these molecules. Their polymerization throughout the volume results in the formation of a continuous silicon–oxygen network and gelation. (We call such a gel a "network" gel as opposed to the colloidal gels considered below.)

The last statement ignores end members of the network. However, this network grows not in a vacuum but inside a water–alcohol solution. Water (and alcohol) and silica are mutually insoluble on the macroscale; hence phase separation between the newly formed silica and water–alcohol is unavoidable. Therefore a two-phase structure is formed. Because water is consumed during the hydrolysis and then again released at polymerization (see Reactions 5 and 6 it should remain in the immediate neighbourhood of the network. This leads to the formation of a porous structure, where the water–alcohol solution is accommodated in pores of diameter 1 to 3 nm with total surface area of 500 to 1000 $m^2 g^{-1}$. Partial phase separation on a macroscale can also sometimes occur; Partlow and Yoldas [111] described many gels (not only in the silica system) which after formation appeared to be immersed in the liquid. We observed several times some excess of a liquid above the well-formed gel.

Two analogies come to mind for qualitative description of this microphase-separated structure. One is a structure of undried leached borosilicate glass, i.e. Vycor-precursor glass. After drying, both materials are able to absorb water actively (in the case of unsintered Vycor the name "thirsty" glass describes this ability). However, as we found by studying the pore structures of "thirsty" Vycor and an acid-catalysed silica gel by nitrogen absorption and mercury porosimetry, Vycor exhibits a much lower BET surface area of 153 $m^2 g^{-1}$ (as against 802 $m^2 g^{-1}$ in one of the gels) and very uniform pore sizes with a diameter of 3.8 nm [112]. The gel shows a much wider pore size distribution with the majority of pores near 2 nm in diameter, but some porosity could be found even in the 10 to 100 nm range.

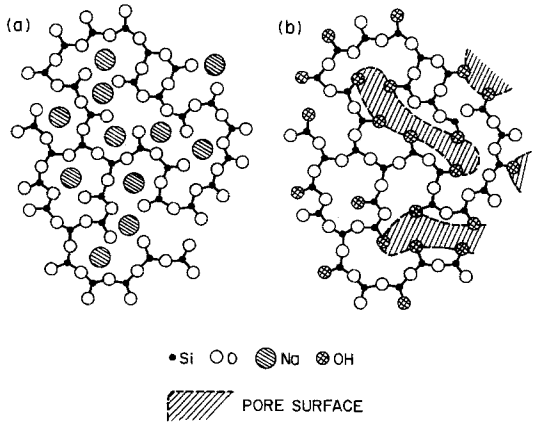

Figure 20 (a) The model of Warren and Biscoe [113] for Na_2O–SiO_2 glass; (b) its modification to describe the structure of an acid-catalysed pure silica gel [112]. Water and alcohol molecules in the pores are not shown.

The second analogy, on the atomic scale, is with the structure of a Na_2O–SiO_2 glass as proposed by B. E. Warren and Biscoe [113] (Fig. 20a). It is clear that the oxygen ions in the silanol bonds are non-bridging oxygens, and the electrostatic role of protons is similar to that of the Na^+ ions in Na_2O–SiO_2 glasses. However there is no geometrical similarity, because the protons of the OH groups are located inside the electron shell of the oxygen ions; the sizes of O^{2-} and OH^- ions are practically the same. Therefore the place of sodium ions is taken by pores (Fig. 20b) hosting water and alcohol molecules, hydrogen-bonded to the silanol groups. Of course, the analogy is only qualitative because the diameter of the pores (about 2 nm) is an order of magnitude larger than the diameter of the Na^+ ions (about 0.2 nm). The water molecule has a diameter of 0.31 nm (the ethyl alcohol molecule has a diameter of 0.46 nm). The 2 nm pore can host only a few water and alcohol molecules in its cross-section, and allows little freedom for structural rearrangement. This probably explains results by W. W. Warren *et al.* [114] and Golding *et al.* [115] who did not observe water crystallization in the silica gel even at liquid nitrogen temperature.

If the water used for hydrolysis has a high pH (above 8, adjusted with NH_4OH), the lack of protons available to form the silanol bonds requires a reduction in the surface area. This results in a complete change of the structure of phase separation with the water–alcohol solution serving as a host to inclusions of silica particles. The precipitation of powder therefore occurs during the hydrolysis–polymerization reactions [116]. The surface area of 100 to 500 $m^2 g^{-1}$ depends on other processing conditions, and it increases with an increase of the amount of water added to the solution [112]. Powders with relatively large particles tend to precipitate, while smaller particles can form a colloidal gel similar to that described in Section 6.1.2.

6.1.1.2. Drying and sintering. The largest part of the volume and mass of a freshly prepared gel is liquid, i.e. water–alcohol solution. If, for example, 4 mol water and 4 mol ethyl alcohol are used for the hydrolysis of 1 mol TEOS, the resulting gel will contain 1 mol silica, 2 mol H_2O and 8 mol C_2H_5OH, i.e. 13 wt % or 5 vol % of silica and 87 wt % or 95 vol % of liquid. The removal of such an amount of liquid from the 2 to 7 nm pores of a "network" gel is the main problem in the preparation of large pieces (at least several centimetres in size) of a sintered gel-derived glass. A very large surface tension developing during the liquid removal by conventional drying forces the network to collapse [117] with the formation of small fragments. Very slow controlled drying yielded relatively small gel pieces [93, 118] which could be sintered in glass, but this method seems to be impractical. The problem of the drying of alkoxide gels has been solved by the technique of hypercritical evacuation in an autoclave [117, 119].

Henning and Svensson [117] described preparation of gel windows of 19.5 cm × 19.5 cm × 3 cm in size (before sintering) from Dynasil M $Si(OCH_3)_4$, methanol, water and NH_4OH as a catalyst. The mixed sol was poured into stainless steel moulds coated with a thin Teflon film. After formation, the gel was covered by a layer of methanol to avoid evaporation and was then washed twice in methanol (during 10 days) to reduce the amount of water to 4%. Then the gel was put in the autoclave and methanol was added and taken to the critical point (240° C, 7.97 MPa for pure methanol). The temperature and pressure programme are shown in Fig. 21. The whole process took 48 h. After reaching the hypercritical conditions and equilibration, the methanol vapour was evacuated at constant temperature with a constant pressure gradient of 0.56 MPa h^{-1}. During the cooling

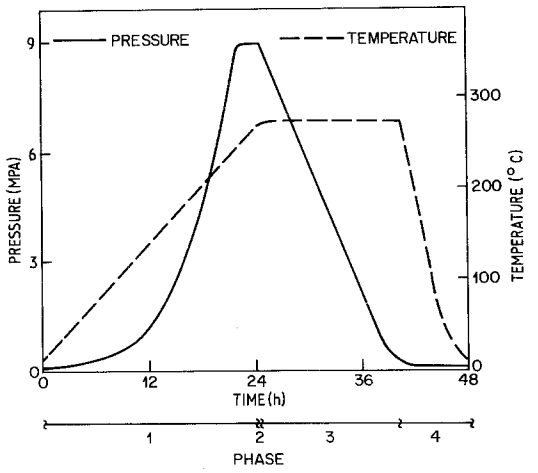

Figure 21 The autoclave cycle for gel drying. The phases of the cycle are (1) heating, (2) equilibrium, (3) vapour outlet, (4) cooling (after Henning and Svensson [117]).

the remaining methanol vapours were flushed out by air.

A similar process has been described by Prassas *et al.* [119]. The main difference is that, in most cases, gelation took place not prior to evacuation, but during the heating in the autoclave. Therefore the formation of porous structure took place during the approach to the critical conditions. A high heating rate was more favourable for successful preparation of monolithic gels, becuse low rates resulted in gelation at lower temperature, far from the critical conditions. The same authors [119] also reported that gels formed before the hypercritical evacuation could be successfully dried.

Sintering of a dry alkoxide gel is a relatively simple process. It can be completed at 800 to 1200° C [7]. One complication is residual carbon in gels – up to 3.4% in the work of Henning and Svensson [117] – because some methoxy groups remain unreacted [119]. However, they can be oxidized by heating in air or oxygen up to 500° C [117]. No details of sintering are given in these studies [117, 119].

Fig. 22 shows the conversion of silica gel to glass for acid and ammonia-catalysed gels [120]. As could be expected, the spherical particles of the ammonia-catalysed gels with larger pores require higher sintering temperatures. The sintering of the "network" gel (HCl-catalysed) is similar to sintering of the "thirsty" Vycor glass.

6.1.1.3. Multicomponent alkoxide gels and glasses. Numerous multicomponent gel-derived

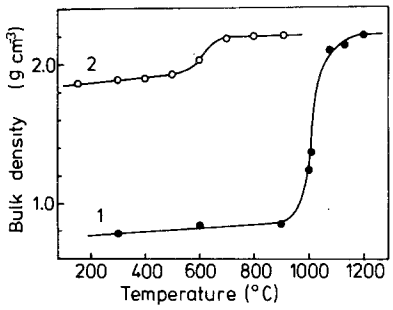

Figure 22 Change in bulk density during sintering of silica gels to glass as a function of temperature for (1) HCl and (2) NH_4OH-catalysed gels (after Nogami and Moriya [120]).

glasses and glass-ceramics have been prepared; a partial list of them is given in Table III. In an earlier period some of the gels were either melted [101] or sintered by hot pressing [102, 103] to prepare monolithic pieces of glass.

Source materials for the addition of other oxides to silica are not necessarily alkoxides; some salts can be used as well (see Table III). In the case of a mixture of different alkoxides (dissolved in alcohols – some of them, such as $NaOC_2H_5$, are powders) the problem is the different rates of their hydrolysis. TEOS is a relatively slowly hydrolysing alkoxide. Therefore, before admixing other alkoxides (e.g. of titanium, aluminium, boron, phosphorus, zirconium or germanium), partial hydrolysis of TEOS must often be conducted [122]. For this purpose 1 mol H_2O is used per 1 mol TEOS and the mixture is held at 50 to 60° C for 1 day. After this other alkoxides and water, sufficient for complete reaction, are added. This results in the formation of a continuous Si–O network modified by other cations (such as sodium, potassium or caesium) and/or comprising other cations (such as boron, aluminium or titanium), similar to that in a melted glass, but with high porosity. Such a gel, when dried, can be sintered to a glass.

A very interesting question is the comparison of the structure of glasses prepared by the gel method with that of glasses of the same composition melted from ordinary batches. There are several works showing significant differences in behaviour of these glasses [101, 136, 142–148]. The difference in rates of crystallization of sintered and melted glasses can be explained by the fact that sintering below the liquidus can be viewed as a latent period of crystallization even if visible crystallization does not occur. When this glass is again heated to the crystallization

TABLE III Multicomponent glasses prepared by the alkoxide gel methods

Glass system	Main source materials*	Authors	Notes
Binary glasses			
SiO_2–B_2O_3,	TEOS, $Si(OCH_3)_4$, $B(OCH_3)_3$, $(NH_4)_2B_4O_7 \cdot 4H_2O$	Yoldas [99], Decottignies *et al.* [102], Jabra *et al* [103], Antonova and D'yakova [121], Woignier *et al.* [122]	(a) In [102, 103] glasses were sintered by hot-pressing
SiO_2–Al_2O_3	sec-$Al(OC_4H_9)_3$	Yoldas [96, 99], Sakka and Kamiya, Negami and Moriya [7], Krol and van Lierop [110]	
SiO_2–P_2O_5	H_3PO_4, P_2O_5, $(NH_4)_2HPO_4$, $P(OCH_3)_3$	Thomas [123, 124], Jabra *et al.* [103], Woignier *et al.* [122]	See Note (a)
72 mol % SiO_2–GeO_2	$Ge(OC_5H_{11})_4$	Fleming [125]	
SiO_2–(20 to 35 vol %) GeO_2	$Si(OCH_3)_4$, $Ge(OC_2H_5)_4$ (produced from $GeCl_4$)	Schlichting and Neumann [126]	(b) Glass films
SiO_2–TiO_2	TEOS, $SiO(OCH_3)_4$, $Ti(OC_2H_5)_4$, $Ti(Oi\text{-}C_3H_7)_4$	Jabra *et al.* [103], Sakka, Kamiya *et al.* [7, 94], Yoldas [127], Yamane *et al* [128] Gonzalez-Oliver *et al.* [129]	See note (a)
SiO_2–(7 and 48 wt %)ZrO_2	$Zr(OC_3H_7)_4$	Kamiya *et al.* [7, 95]	(c) Glass fibres
SiO_2–(1 to 40 mol %)Na_2O	TEOS, $Si(OCH_3)_4$, $NaOCH_3$	Puyane *et al.* [130], Prassas *et al.* [131, 132]	
$CaO \cdot 4\ SiO_2$, $CaO \cdot 9\ SiO_2$	$Ca(OC_2H_5)_2$ (from Ca + ethanol reaction)	Hayashi and Saito [133]	
SiO_2–(1, 5, 10 wt %)SrO	$Sr(NO_3)_2$	Yamane and Kojima [134]	(d) Homogeneous glasses were prepared which could not be prepared by melting due to phase separation at 3 to 30 wt % SrO.
SiO_2–(5 to 40 wt %)Fe_2O_3	$Fe(OC_2H_5)_3$	Guglielmi and Principi [135]	
Ternary Glasses			
SiO_2–(5 to 30 wt %)La_2O_3 80 to 85 wt % SiO_2, 10 La_2O_3, 5 to 10 Al_2O_3 80 to 94 wt % SiO_2, 5 to 10 La_2O_3, 1 to 10 ZrO_2	Method I: Silica hydrosol Ludox AS, $La(NO_3)_3$, $Al(NO_3)_3 \cdot 9\ H_2O$, $ZrOCl_2 \cdot 8\ H_2O$ Method II: TEOS, $Si(OCH_3)_4$, $La(NO_3)_3$, $Al(Oi\text{-}C_3H_7)_3$, $Al(OC_4H_9)_3$, $ZrOCl_2 \cdot 8H_2O$	Mukherjee *et al.* [101, 136], Decottignies *et al.* [102]	(e) Gels were melted to yield glasses in [101]; see also Note (a)
60 to 76 wt % SiO_2, 17 to 33 ZrO_2, 7 Na_2O	$Zr(OC_3H_7)_4$, $NaOCH_3$	Kamiya *et al.* [7, 95]	See note (c)

Continued

TABLE III *Continued*

Glass system	Main source materials*	Authors	Notes
SiO_2–B_2O_3–P_2O_5	$Si(OCH_3)_4$, $B(OCH_3)_3$, $P(OCH_3)_3$	Woignier *et al.* [122]	
SiO_2–MgO–Al_2O_3, Al_2O_3/MgO mol ratio 0.5, 0.71, 1.3 with or without additions of TiO_2 (up to 10 wt %) and Li_2O (5.5 wt %)	$Al(OC_4H_9)_3$, $(CH_3COO)_2Mg \cdot 4H_2O$, $(CH_3COO)Li \cdot 2H_2O$, $Ti(OC_2H_5)_4$	Höland *et al.* [137]	(f) Glass–ceramics
40 to 80 mol % SiO_2, 4 to 64 Al_2O_3, 4 to 64 CaO	sec-$Al(OC_4H_9)_3$, $Ca(NO_3)_2$	Pancrazi *et al.* [138]	
SiO_2–TiO_2–ZrO_2	$Ti(OC_4H_9)_4$, $Zr(NO_3)_4 \cdot 5H_2O$	Zhu Chongshen *et al.* [139]	
(73.5 to 74.25 wt %) SiO_2, (0.5 to 8.25) CaO, (17.75 to 25.25) Na_2O	$Ca(OC_2H_5)_2$, $Na(OC_3H_7)$	Yoldas [98]	
55 wt % SiO_2, 25 B_2O_3, 20 Na_2O	H_3BO_3, $B(OCH_3)_3$, $NaOCH_3$	Mukherjee [140]	
Multicomponent glasses			
66 wt % SiO_2, 18 B_2O_3, 7 Al_2O_3, 3 BaO, 6 Na_2O	$B(OCH_3)_3$, $Al(OC_4H_9)_3$, $Ba(OC_2H_5)_2$,	Brinker and Mukherjee [92, 141]	
86.9 wt % SiO_2, 5.9 B_2O_3, 2.5 Al_2O_3, 3.9 Na_2O, 0.7 K_2O	$Si(OCH_3)_4$, H_3BO_3, Sec-$Al(OC_4H_9)_3^g$, $NaOCH_3$, KOC_2H_5	Dislich [89]	(g) glass–ceramic films, nucleation temperature of 680° C, crystallization temperature 830° C
61.4 wt % SiO_2, 21.6 Al_2O_3, 6.8 P_2O_5, 3.8 Li_2O, 1.4 MgO, 0.5 Na_2O, 2.6 TiO_2, 1.9 ZrO_2			
62 wt % SiO_2, 21.9 Al_2O_3, 2.8 Li_2O, 1.1 MgO, 1.8 TiO_2, 1.8 ZrO_2, 6.2 ZnO, 1.6 BaO, 0.5 CaO, 0.4 K_2O	Not given		
75 wt % SiO_2, 16.5 Al_2O_3, 4.7 Li_2O, 1.8 TiO_2, 1.5 ZrO_2, 0.5 Na_2O†	Not given	Yoldas [98]	(h) glass–ceramic composition
Non-Silicate Oxide Glasses			
P_2O_5–Na_2O	$PO(OC_2H_5)_3$, $NaOCH_3$	Gottardi [142]	
B_2O_3–(14.2 and 17.9 wt %) Li_2O	*n*-$B(OC_4H_9)_3$, $LiOCH_3$	Weinberg, *et al.* [143]	

*When $Si(OC_2H_5)_4$ (TEOS) is the only source of SiO_2 in a gel, it is omitted from this column.
†We corrected this composition, which is given in [98] with obvious misprints.

temperature it will crystallize more rapidly than a piece of the melted glass.

Mukherjee and co-workers [101, 136] observed a difference in the crystallization of gel-derived and batch glasses in the SiO_2–La_2O_3 system even after these glasses were remelted. In part this can be explained by different amounts of alkali impurities drastically enhancing crystallization (one of the source materials for gel, Ludox, has these impurities) or by a different OH content, which is usually higher in gel glasses. Weinberg and Neilson [145–148] even found different liquidus temperatures in gel and batch glasses (both remelted) of the same composition in the Na_2O–SiO_2 system. They explained this difference by a different OH content (0.009% in the gel glass compared with 0.005% in the batch glass). We doubt whether this low OH content could account for the change in the liquidus temperature. Studying lithium borate glasses, Weinberg *et al.* [143] did not detect any difference in the behaviour (including crystallization) between gel-sintered, gel-remelted and batch-melted glasses of the same composition when the gels were thoroughly dehydrated.

6.1.2. Colloidal gels

Shoup and Wein [149, 150] prepared porous gel bodies from mixtures of sodium or potassium silicate (8.3 wt % K_2O and 20.8% SiO_2) and colloidal silica sol Ludox containing ~40 wt % SiO_2. The mixture of these two materials with formamide was gelled and then leached in weak acid solutions or NH_4NO_3 solutions to reduce the alkali content to < 0.02%. The sol showed 13 to 25% linear shrinkage during gelation. The gel consisted of spherical particles of 30 to 180 nm in diameter. The average pore diameter of the gel decreased with an increase in the amount of Ludox, and could be in the range 10 to 350 nm. Every one of these gels possessed a relatively narrow pore size distribution. As seen, pores in this kind of gel are one or two orders of magnitude larger than those in alkoxide gels. Such structures are capable of withstanding capillary forces at drying. In this way relatively large articles could be formed and sintered to a transparent glass.

Rabinovich *et al.* [151–157] developed a method of preparation of high-silica glass (96 to 100 wt % SiO_2, 0 to 4% B_2O_3) from commercial silica Cab-o-Sil (Cabot Corporation) prepared by reacting $SiCl_4$ in a flame. The material has a BET surface area of 230 $m^2 g^{-1}$ and a low impurity level [151, 152]. When dispersed in water or aqueous solution of H_3BO_3, this material forms a sol of pH 2.7. (It was difficult to disperse more than 68 g of the silica in 100 g H_2O.) When poured into a stoppered silica tube this sol gelled in 1 to 2 h and was able to maintain its shape without a mould. The gelation was reversible and, if the gel was mixed again prior to drying, it returned to the sol state. Drying resulted in fracture similarly to that with alkoxide gels.

To produce large gel articles without fracture the so-called "double" processing was invented [152, 155]. The first sol was dried and formed relatively dense pieces (note that the original Cab-o-Sil is a fine fluffy powder) still with the unchanged surface area, which remained practically the same even if the pieces were heated at between 300 and 900° C. This secondary material, when redispersed again in a high-shear device (e.g. a blender), again formed a sol and a gel which could now be easily dried without breaking. Porous tubes up to 40 cm long and 3.8 cm diameter and rods of various sizes could be prepared.

An extensive study of gels by the method of mercury porosimetry coupled with an agglomerate study with a Coulter counter [152] and by infrared spectroscopy [154] revealed the details of gel formation. Every spherical colloidal silica particle (about 13 nm in diameter) has silanol groups on its surface, or they formed by reaction of the superficial siloxane groups with water. Wood *et al.* [154] found that these groups adsorb H_2O molecules by hydrogen bonding during dispersion. These particles are able to move freely in the liquid phase. However, on standing, the suspended particles may associate through spontaneously formed hydrogen bonds between silanol groups on one particle and siloxane groups on another. Thus the rigid network is formed. This initial process can be visualized as in Fig. 23 [154].

When the initial particles are joined, neck growth occurs around the contact point as described by Iler [108]. Silica is dissolved from the exterior of the particles and deposited in the neck region. Joining of other particles causes the formation of chains and eventually a three-

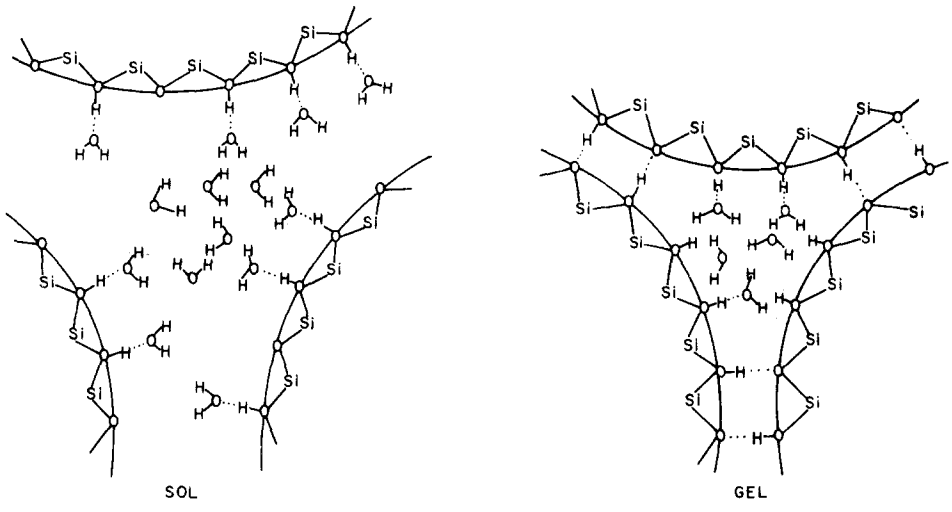

Figure 23 Structural diagram of atomic-level changes during gelation of a colloidal (Cab-o-Sil) sol. Dots represent hydrogen bonds, and curved lines represent micelle surfaces (after Wood *et al.* [154]).

dimensional structure. The sol hardens to a gel [152].

Redispersion results in a partial destruction of the necks, and the fluidity is restored. However not all the necks are destroyed, and the new sol consists of aggregates. The structure of the second gel can be represented as in Fig. 24 [152]. The relatively large pores between the aggregates provide convenient paths for water removal, and this gel can be easily dried. The scheme of Fig. 24 was confirmed by electron microscope study and by mercury porosimetry [152]. The latter method showed a two-mode pore size distribution curve: one maximum in the region 1 to 8 μm (inter-aggregate pores) and the second one in the region 13 to 20 nm (intra-aggregate pores).

The overall scheme of preparation of transparent high-silica is shown in Fig. 25 [152]; the detailed study of sintering of these glasses has been described [153]. The dynamic sintering results are shown in Fig. 26. The isothermal shrinkage data were also studied and Fig. 27 demonstrates their fit with Scherer's model [21], described in Section 2. As seen, reasonably good fits were obtained up to $\varrho/\varrho_s = 0.5$; after that the fit was poor. Apparently Scherer's assumption [21] that the structure of a colloid before sintering is approximated by an array of glass cylinders is not quite true for the combination of aggregates shown in Fig. 24. Calculated

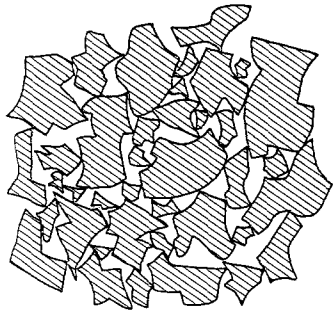

Figure 24 Schematic drawing of the microstructure of twice-dispersed colloidal silica (after Rabinovich *et al.* [152]).

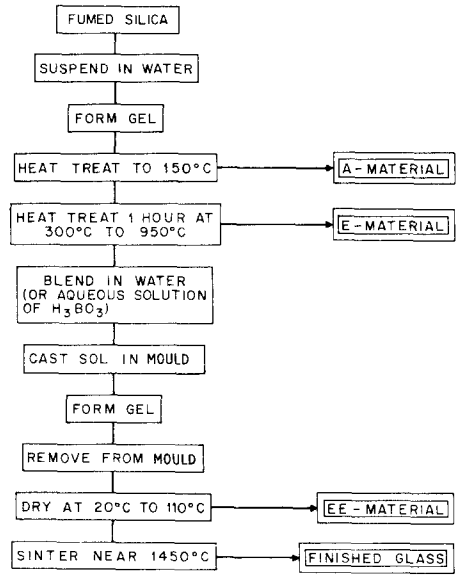

Figure 25 Process chart for the preparation of transparent glass from colloidal gels (after Rabinovich *et al.* [152]).

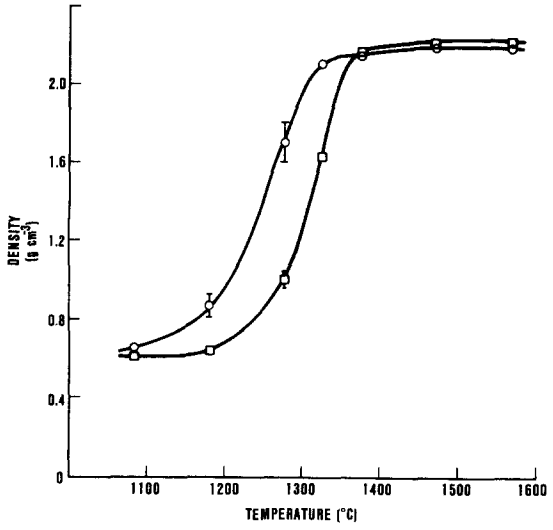

Figure 26 Density of gel-derived glasses as a function of temperature for 400° C h^{-1} heating in air (after Johnson *et al.* [153]). (□) SiO_2; (○) 97 wt % SiO_2, 3% B_2O_3.

activation energies of viscous flows for sintered gel-derived glasses were 598 kJ mol^{-1} (100% SiO_2) and 460 kJ mol^{-1} (3% B_2O_3), which are close to values for commercial silica glasses. However, values of the viscosity calculated from the sintering data were high by more than one order of magnitude [152].

Pieces of these glasses were sintered to essentially bubble-free glasses in the atmosphere with Cl_2 added (to dehydrate glass) at 1450 to 1550° C during 15 min (heating rate ~ 400° C h^{-1}). However these glasses had some bubbles and other defects, apparently due to large pores [153]. In a later work Rabinovich *et al.* [156] reported that a new (unspecified) method for the second dispersion resulted in reduction of the larger pore sizes, and provided defect-free glasses by sintering at as low as 1260 to 1300° C. Dehydration by chlorine resulted in an OH level below 1 ppm. Tubes up to 25 cm long with 2.3/1.7 cm outside/inside diameter were produced by this method (Fig. 28). Properties of these gel-derived glasses were similar to those of commercial silica [151, 152], although the modulus of rupture was somewhat lower if fire polishing had not been applied.

Scherer and Loung [158] reported the preparation of colloidal gels from silica particles 60 to 100 nm in diameter (surface area 27 to 45 m^2 g^{-1}) produced by flame oxidation of $SiCl_4$. The particles were dispersed in organic liquids such as chloroform or n-decanol with the additions of amines or ammonia. Because much larger particles were taken than in work by Rabinovich *et al.* [151–157], double processing was not necessary (it is difficult to gel such relatively large particles in aqueous solutions). The dried gels were sintered at 1450° C in an He/Cl_2 atmosphere. A glass rod of 1.3 cm in diameter and 7 cm long was prepared by this method; the OH content was below 1 ppm. The process of sintering could be well described by Scherer's model [21].

Sacks and Tseng [159, 160] described the preparation and sintering of silica glass from powder compact. The powders were prepared by hydrolysis of TEOS in the presence of ammonia – a method similar to that used by Shimohira *et al.* [25] (see Section 2). The resulting particles [159, 160] were relatively large and uniform in

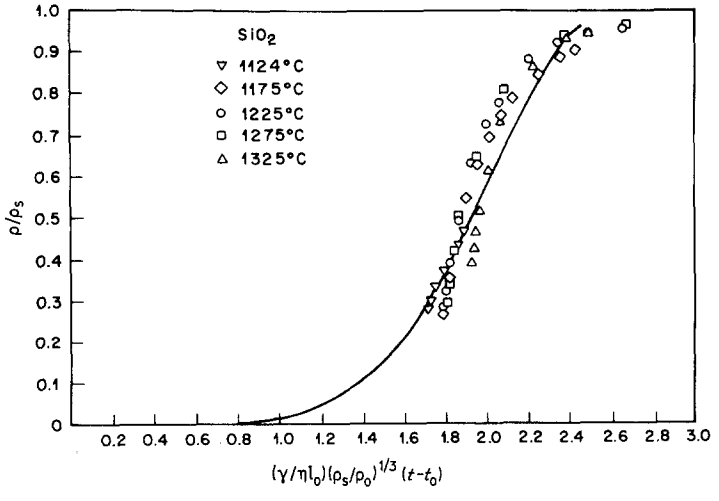

Figure 27 Fit of isothermal shrinkage data for gel-derived SiO_2 to sintering model [22] (after Johnson *et al.* [153]).

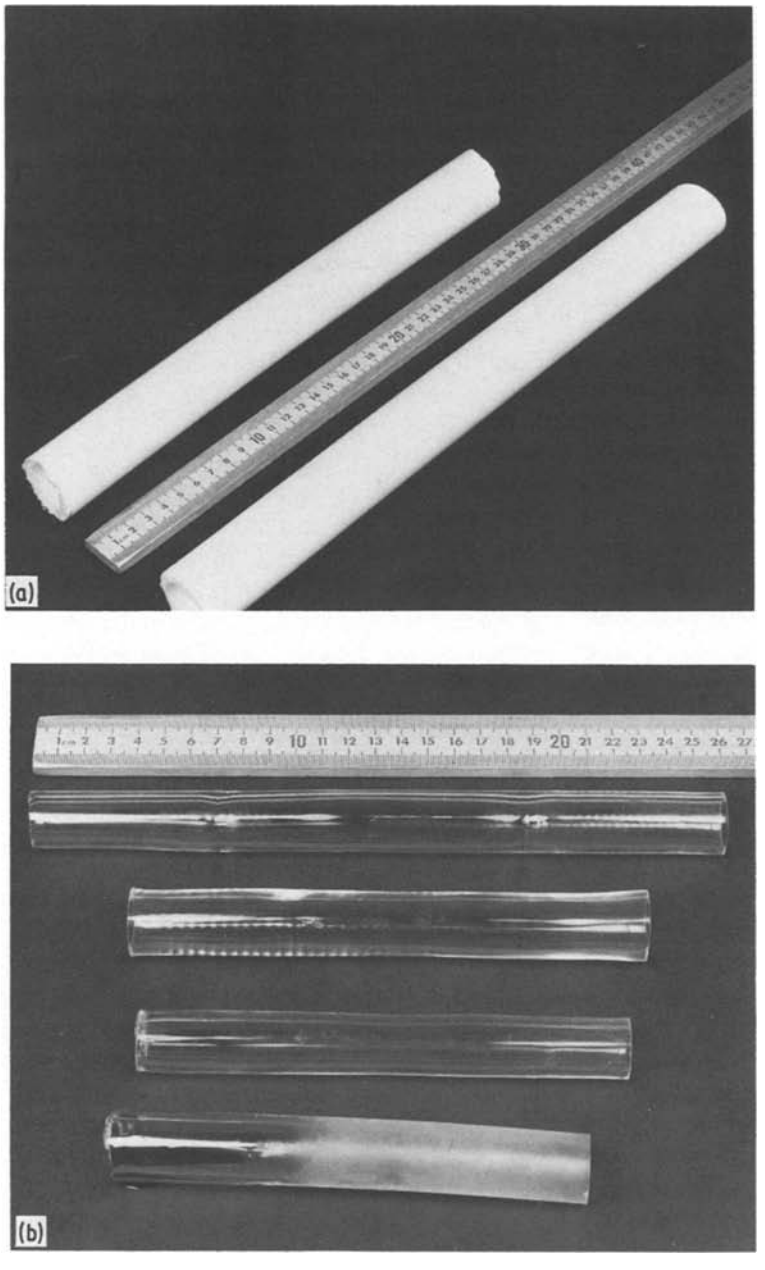

Figure 28 Colloidal silica gel tubes (a) before and (b) after sintering. Glass tubes are fire-polished, except the bottom one, the left end of which is coated with glycerine to remove surface haze (after Rabinovich *et al.* [156]).

size (0.2 to 0.6 μm depending on conditions of preparation) with a surface area near 7.5 $m^2 g^{-1}$. The highly ordered compacts were prepared by precipitation of the powders and then sintered in the range from 900 to 1050° C. The process of sintering was found to conform to the models of Mackenzie and Shuttleworth [11] and of Scherer [21]. However, only small (0.8 cm diameter and 0.08 cm thick) translucent rather than transparent specimens could be prepared by this method [159, 160] at 1000° C. The use of higher sintering temperatures resulted in devitrification.

Table IV outlines the main differences between alkoxide network and colloidal gels. One of the main problems with colloidal gels is the introduction of components other than silica. It is relatively easy with alkoxides, but much more difficult with colloidal silica. As was shown above, B_2O_3 can easily be introduced by using an H_3BO_3 solution [151–153]. Some success was reported by Rabinovich *et al.* [157] with other

TABLE IV Comparison of alkoxide network gels and colloidal gels

Alkoxide network gels	Colloidal gels
Gelation is a result of chemical reaction and is irreversible	Gelation is a result of hydrogen-bond formation between colloidal particles and a liquid and is reversible (thixotropy)
Glass-like network is formed during gelation at room or slightly elevated temperature	Continuous glass network is formed only at sintering
Porous structure of the unsintered dried gel resembles that of a non-sintered "thirsty" glass (Vycor)	Porous structure is defined by random packing of spheres and shapeless aggregates

glass formers such as P_2O_5 and GeO_2. However Al_2O_3, TiO_2, ZrO_2 and their compounds form crystalline or easily crystallizing oxides and provoke crystallization of glass during sintering below the liquidus. Meissner and Stookey [161] patented the preparation of gels from colloidal solutions with soluble silicate (of sodium and potassium) and their successful sintering into glass.

Mazdiyasni [162] described methods of chemical synthesis of single- and mixed-phase oxide ceramics. If every particle has the same multicomponent composition, then colloidal methods can be applied to the preparation of complex glasses. However, pores in colloids are usually larger than in alkoxide network gels. This results in higher sintering temperatures (e.g. 1300° C for colloidal SiO_2 compared with about 1000° C for alkoxide SiO_2) which takes a glass into the active crystallization range. Pure silica glass has one of the lowest rates of crystallization, and it is not easy to find an addition to this glass (in a high-silica region) which will not cause crystallization, even when it is present as a part of the silicon-oxygen network. One of the few exceptions is probably Al_2O_3: glasses in the Al_2O_3-SiO_2 system with $Al_2O_3 \leqslant 5$ wt % do not crystallize up to 1400° C [7].

6.1.3. Application of gel-derived glasses

Except for the relatively old and established application of alkoxide gels to thin films deposition [7, 89], we do not yet know any industrial application of the sol–gel processes. However, the intensity of research in this area and the promise of the methods are so high that this statement may become obsolete even before this review is published. The advantages of sol–gel processes are: (a) preparation of glasses at temperatures significantly below the conventional melting temperatures (compare 1000 to 1450° C for silica glass prepared by different gel methods with 1800 to 2000° C for fused silica); (b) relatively simple equipment and low capital investment due to the absence of glass melting kilns – this also provides the possibility to produce glasses of different compositions in the same equipment and easy switching of compositions; (c) very high homogeneity of glass [88] because the mixing takes place in solution; (d) the use of purified reagents and the absence of contact with a container in the melted state provides a high purity of the resulting glass (some reservations relating to this statement will be considered below); (e) the possibility of producing unique glasses which cannot be produced by melting due to crystallization or phase separation (e.g. SrO–SiO_2 glasses, see Table III [134]), or simply because melting temperatures are too high. However, it remains to be seen how large the fabricated articles can be when made by a sol–gel process.

Several applications are widely discussed in the literature. Henning and Svensson [117] used their method of monolithic gel preparation in an autoclave to produce Cerenkov radiators with a refractive index of 1.01 to 1.06; aerogels prepared by them (see Section 6.1.1.2) had just this range of indices due to high porosity. However, this was a rather limited application for scientific purposes.

Recently a short note appeared [163] that "researchers at Lawrence Berkeley Laboratory in California have begun a project to see if transparent, microporous materials, called aerogels, can be used to build insulating windows". They intend to explore supercritical drying to prepare windows 2.54 cm thick with an insulation value equal to 7.62 cm of fibre-glass batting.

One of the most interesting applications of the sol–gel process is the production of fibres, especially of optical fibres. Susa *et al.* [164] demonstrated the feasibility of this approach. They prepared an alkoxide-derived silica rod, slowly dried it and sintered it at 1200 to 1300° C. This rod was used as the core material in optical fibre

preparation. The rod was put in a tube and a boron-doped silica glass cladding was deposited by chemical vapour deposition (apparently by the MCVD method, see Section 6.2.1 below). The transmission loss of the optical fibre drawn from this preform was 6 dB km^{-1} at a wavelength of 0.85 μm.

Rabinovich *et al.* [156] reported an optical fibre prepared by the MCVD process with the colloidal (Cab-o-Sil) gel-derived silica glass tube (25 cm long, 2.3/1.7 cm outside/inside diameter) used as a substrate. The tube was fire-polished in an atmosphere of helium and Freon 12, and an SiO_2-P_2O_5-F cladding and an SiO_2–GeO_2 core were deposited. The tube was collapsed and the fibre was drawn with 150 μm total diameter and a core of 8.6 μm; the refractive index difference was $\Delta n = 0.0045$. This fibre showed a minimum loss of 0.7 dB km^{-1} at 1.15 μm, but the light-guiding part of the fibre was not gel glass. A gel-derived silica rod with silicone polymer cladding gave a loss of 50 dB km^{-1}, but no special precautions had been taken to ensure high purity of the glass. (A recent, more advanced fibre with a gel-derived tube serving partially as an outer cladding is described in Section 6.2.1.)

It is interesting to compare this method [156] with that of Scherer and Loung [158], although no gel-derived fibre was described in the latter paper. Both methods provide glasses of comparable purity with the same very low OH content. Scherer and Loung used gelation of colloidal silica of relatively low surface area, which allowed them to avoid "double processing" for the preparation of uncracked bodies. This seems to be advantageous. However their liquids (decanol and chloroform) are much more expensive than the deionized or distilled water used by Rabinovich *et al.* [152]. Besides, chloroform is a dangerous substance and a cancer suspect [165]; this alone may introduce significant cost additions to provide safety, and may offset the potential economical advantage of the simpler processing.

Harmer *et al.* [166] described another method of optical fibre fabrication from gels. An alkoxide solution is introduced into a vertical silica tube and drains out slowly, leaving a thin film inside. After gelation, drying and curing during 30 min, the next layer is applied. They compared this process with the successive layer deposition in the MCVD process. In this way they fabricated 0.5 km of fibre with an 8% GeO_2-doped core with a loss of 22 dB km^{-1} at 0.85 μm. The high loss was attributed to transition metal impurities in the $Ge(OC_2H_5)_4$.

The same authors [166] provided some preliminary calculations of production cost for 100 000 km per year of a 50/125 μm fibre with TiO_2 used as a dopant. They compare these calculations with similar calculations for the VAD process (described in Section 6.2.1). The production cost estimate (not including testing, sorting and packaging) is 12 compared with 52 US$ per km of the fibre for VAD. Harmer *et al.* [166] did not take into account that it is more difficult to provide a high degree of purity in any gel process than in any vapour deposition process. The steps necessary to provide this purity can significantly add to the cost.

Other kinds of glass fibres also can be produced by gel methods. Sakka [7] wrote that when 1 to 2 mol H_2O per 1 mol of an alokoxide are used, acid catalysed gels can exhibit spinnability during their polymerization. Both Sakka *et al.* [7] and LaCourse *et al.* [167, 168] described fibres from such gels which could be sintered to glass fibres. However, the strength of these fibres is significantly lower than that of fibres drawn from a melt [168].

Glass tubes and other bulk glass materials can be produced by gel methods. We think that colloidal gel processes for pure silica or high silica glasses [149–161] may eventually replace the more complicated Vycor process (see Section 4).

6.2. Deposition from the vapour phase for optical fibre fabrication

6.2.1. General description

The concept of the transmission of messages by light is not new. "And what I watched for is a beacon fire, a flash of flame to bring the word from Troy, word that the town has fallen," tells a watchman in Aeschylus' "*Agamemnon.*" Of course, he expected not a real "word" but a signal, the meaning of which was prearranged. Yet it took until 1880 when A. G. Bell invented the photophone [4] for speech to be transmitted by light. Bell used the sun as a light source and the atmosphere as the transmission medium; both are unreliable. The invention of the laser in the late 1950s rekindled the interest in communication by light, but a reliable transmission

medium was needed. Fibre optics based on glass were proposed by Kao and Hockham in 1966 [169], and by 1970 low losses were reported by Kapron *et al.* [170]. In the 1980s, lightwave transmission systems are a reality.

A review of the whole concept was given by Pearson *et al.* [4]; MacChesney [171] and Schultz [5, 6] recently reviewed the state of the art in optical fibre fabrication. Several books have been published on this subject [172, 173]. A detailed review of this complex problem is outside the scope of this paper. We shall briefly recall the concept and the main technological principles, and then consider publications dealing with the sintering of optical fibre preforms.

A lightwave communication system consists of three major components [4]: light source, transmission medium, and the receiver containing a photodetector. A fibre lightguide is used as a transmission medium. Fig. 29 illustrates how light is transmitted by total internal reflection. The cladding has a lower refractive index than the core in a lightguide structure. Three types of the fibre are single-mode, multimode step index, and multimode graded index [4]. The condition for single-mode operation [4] is

$$\frac{2\pi a}{\lambda}(2n\Delta n)^{1/2} \leqslant 2.41 \qquad (7)$$

where a is a core radius, λ the wavelength, n the core refractive index and Δn the difference in refractive indices between core and cladding. For $\lambda = 0.8\,\mu m$, $n = 1.47$ (fused silica) and $\Delta n = 0.01$, the maximum core diameter is $2a = 3.5\,\mu m$. At larger cores the fibre transmits lights like a multimode.

A major property of interest in these glass fibres is the optical attenuation, which is measured in $dB\,km^{-1}$. For long-distance communications the loss should be below $5\,dB\,km^{-1}$ [4]. Intrinsically, attenuation in glasses is caused by absorption due to electronic transitions and molecular vibrations, and Rayleigh scattering due to density and concentration fluctuations. These phenomena are at a minimum in the near infrared region of the spectrum. However, extrinsic sources of optical attenuation such as scattering due to inhomogeneities and absorption primarily due to impurities of transition metals and water must be tightly controlled.

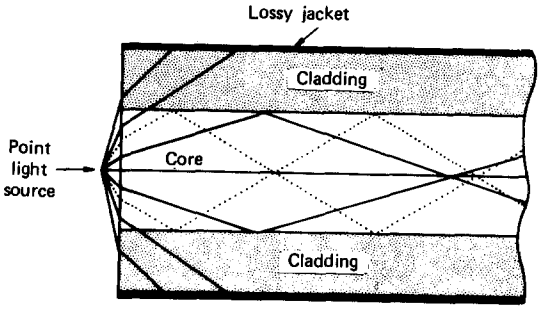

Figure 29 Light from a point source collected and guided by a glass fibre lightguide (after Pearson *et al.* [4]).

Early research on optical fibre preparation used technology similar to that for continuously fabricated strands of fibres [1, 4] except that double-crucible techniques were employed [4]. Various ways of preparing ultra-high purity multicomponent glasses were tried, and significant but insufficient progress in reduction of the attenuation was reported (down to $12\,dB\,km^{-1}$). However, the real breakthrough occurred when flame hydrolysis and chemical vapour deposition processes were used. Their emergence coincided with the conclusion that high-silica compositions rather than multicomponent glasses were the materials of choice because they showed very low optical attenuation in the near infrared region of the spectrum [4, 169].

The very high temperature for melting silica required new methods for its preparation. At the same time it became clear that liquid silicon tetrachloride ($SiCl_4$) is a desirable raw material, because it is much more volatile than transition metal halide impurities; it can therefore be vapour entrained and then hydrolysed or oxidized in the vapour phase, yielding very pure fine amorphous silica particles [171]. Hyde [174] showed that these particles (soot) can be vitrified to bubble-free glass at temperatures below the liquidus.

Fig. 30, derived from reviews by MacChesney [171] and Schultz [5], shows the three main processes currently used worldwide to produce optical fibres. In Corning's Outside Vapour Phase Oxidation (OVPO) process* (Fig. 30a), $SiCl_4$ mixed with dopants (e.g. $GeCl_4$) is hydrolysed in a gas–oxygen burner to produce a stream of fine particles. These particles are deposited on a rotating mandrel. When a sufficiently

*Schultz [5] calls this process Outside Vapour Deposition (OVD).

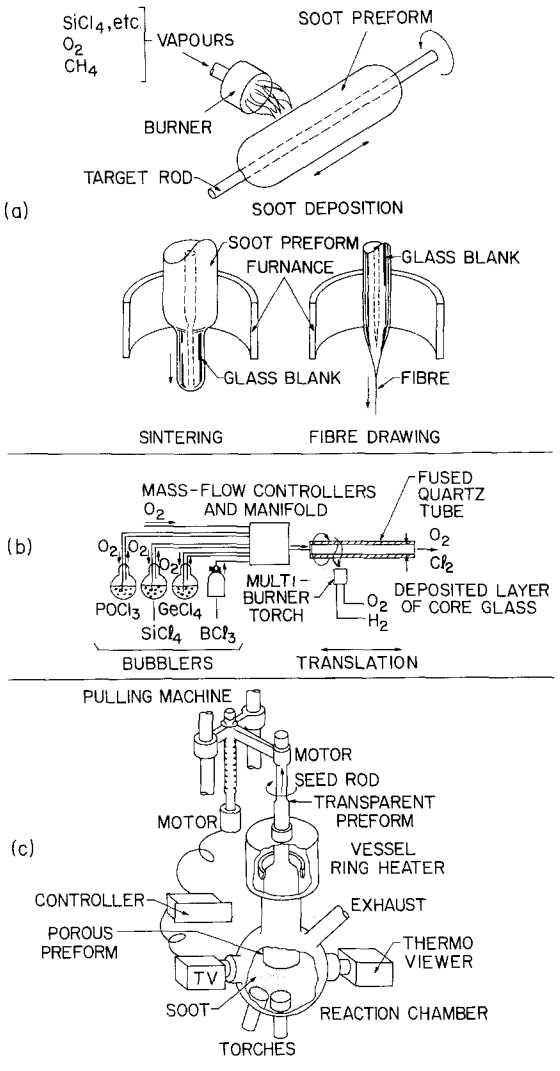

Figure 30 Processing scheme for the preparation of optical fibres: (a) OVPO process developed at Corning Glass Works (after Schultz [5]); (b) MCVD process of AT & T Bell Laboratories; (c) VAD process developed in Japan. (b) and (c) are after MacChesney [171].

thick layer is formed, another layer with a composition to yield a lower refractive index glass is deposited. The mandrel is then removed, and the porous preform is sintered to a glass blank which, in its turn, is drawn to produce a fibre. During the sintering, but prior to pore closure, a chlorine treatment results in the reduction of OH contamination to less than 0.1 ppm [5, 6]. The characteristics of fibres thus produced are presented in Table V.

The Chemical Vapour Deposition (CVD) method consisted of the direct deposition of a thin glassy layer on the inside wall of a quartz tube as a result of heterogeneous reaction of SiH_4, GeH_4 etc. with O_2 or CO_2 near the tube's wall [171]. However, the method was limited to low deposition rates. Attempts to increase the rate of supply of the reagents resulted in homogeneous reactions with formation of particles which were incorporated into the glass layer and produced defects.

A modification of this method called Modified Chemical Vapour Deposition (MCVD) proved to be a great technical and commercial success. The method, described in Fig. 30b, was invented by MacChesney *et al.* [171, 175–179] at Bell Laboratories. The reagents are chlorides, such as $SiCl_4$ and $GeCl_4$, and they predominantly react homogeneously with oxygen in the gas phase to produce silica or doped SiO_2 particles. These particles are deposited on the tube walls by thermophoresis and are subsequently vitrified by sintering. In the MCVD process, first the cladding material and then the core is deposited. An external torch travelling along the length of the rotating tube provides the thermal energy to sinter each deposited layer (at 1600 to 1900° C). Upon completion of the deposition, the tube is collapsed by heating to higher temperatures to form a glass preform (blank) from which the fibre is drawn.

Over the past decade the MCVD process has been perfected to become a large-scale manufacturing process. Because the reaction takes place inside the closed tube, clean-room conditions are unnecessary to maintain high purity. The thermophoretic mechanism of particle deposition has been established [179]. Its mathematical modelling (by Walker *et al.* [180]) predicted the deposition efficiency in terms of process variables. The radio-frequency plasma MCVD process [181] achieves very high deposition rates by maximizing these phenomena. The rate of the deposition in the MCVD process has been increased from about $0.2\,g\,min^{-1}$ in 1974 to $2.3\,g\,min^{-1}$ in 1982, while the plasma method achieved the rate of $6\,g\,min^{-1}$ in 1983 [182, 183].

The third major lightguide fabrication method (Fig. 30c) is Vapour-phase Axial Deposition (VAD), first reported by Izawa *et al.* [184, 185]. It is somewhat similar to OVPO, because it is an outside soot process. However the soot is deposited on the end of a rotating mandrel, thus eliminating the central hole. The porous preform can be pulled up through a ring

TABLE V Examples of optical fibres prepared by the OVPO (OVD) method, after Schultz [5]

Example	A	B	C
Numerical aperature	0.2	0.3	0.3
Core diameter (μm)	50	100	100
Fibre diameter (μm)	125	140	140
Core glass system	GeO_2–P_2O_5–SiO_2	GeO_2–B_2O_3–SiO_2	GeO_2–SiO_2
Clad glass system	SiO_2	B_2O_3–SiO_2	B_2O_3–SiO_2
Attenuation (dB km^{-1})			
820 nm	2.5	4.0	4.0
1200 nm	0.6	2.0	1.5
1300 nm	0.7	3.0	1.5
1500 nm	0.8	–	2.0
1600 nm	0.3	–	2.5
ppm OH	< 0.1	< 0.1	< 0.1
Bandwidth (MHz km)	> 1000	> 200	> 20

heater in which sintering of the previously deposited material takes place in the presence of Cl_2, while deposition continues at the bottom. The process can be monitored and controlled using feedback from a TV camera. Lightguides of excellent performance have been achieved with this process, and it has the potential for operation in a continuous mode.

All three methods are compared in Table VI, compiled by Nagel *et al.* [179]. The loss is shown for multimode fibres only. Losses as low as 0.16 dB km^{-1} have been achieved in single-mode fibres [186]. In a recent experiment [187] light was transmitted error-free at 420 MB sec^{-1} in such a fibre over distances of 203 km. This compares with a typical repeater spacing for modern coaxial cable systems of 9 km [171].

All three methods use GeO_2 and P_2O_5 dopants to increase the refractive index, and B_2O_3 to decrease the index. Recently fluorine doping to decrease the refractive index has become important [188, 189]. As mentioned in Section 6.1.3, tubes were fabricated by a colloidal (Cab-o-Sil) gel method used in conjunction with the MCVD process (MacChesney *et al.* [190]). Fluorinated and dehydrated colloidal gel substrate tubes were prepared to match the refractive index of fluorosilicate claddings. This eliminated leaky-mode effects and reduced the amount of deposited cladding required by at least a factor

TABLE VI Comparison of optical fibres produced by different methods, after Nagel *et al.* [179]

Parameter	OVPO	MCVD		VAD
		Standard	Plasma	
Numerical aperture (NA):				
typical	0.2	0.23	0.23	0.2
maximum reported	0.3	0.38	–	0.32
Deposition rate (g min^{-1}):				
typical	1.5 to 2	0.35 to 0.5	3.5	0.3 to 0.5
maximum reported	4	1.3	5.0	2
Efficiency (%)	50	50	80	60
Maximum blank length reported (km)	40	40	> 20	100
Best multimode results for fibre with NA;	0.21	0.23	0.2	0.21
loss (dB km^{-1}) at				
0.82 μm	2.5	2.6	2.8	2.5
1.3 μm	0.7	0.45	0.7	0.42
1.5 to 1.6 μm	0.8	0.35	0.5	0.31
Bandwidth (GHz km)	> 3	5	–	6.5
Min. OH(ppb)	10	3	10	1

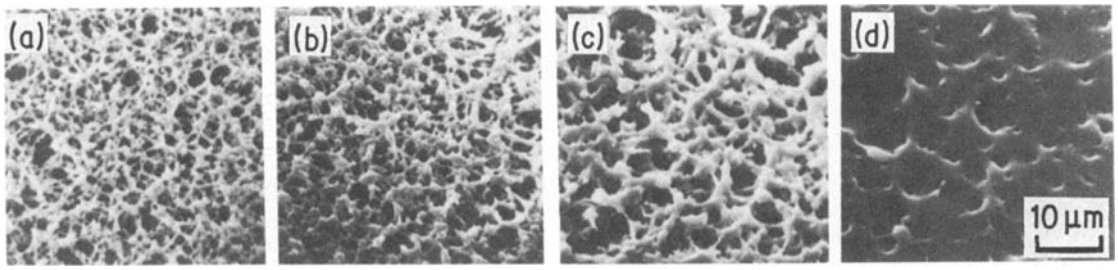

Figure 31 Micrograph (top views) showing consolidation of a GeO_2–B_2O_3–SiO_2 layer at progressive locations of the MCVD tube in the axial direction: (a) 0 sec, 700° C; (b) 1 sec, 1200° C; (c) 2 sec, 1600° C; (d) 3 sec, 1600° C. The temperature gradient in the tube was about 300° C cm^{-1}; helium was admixed with O_2 (after Walker *et al.* [191]).

of four. The ratio diameters of the deposited cladding to core was 4.5. The core was of a GeO_2–SiO_2 composition, and the silica cladding was doped with fluorine. The light field travelled in the deposited core and cladding, but leaky-mode losses from tunnelling to the higher-index outer cladding (the substrate tube) were prevented. The single-mode fibre prepared using such a tube exhibited a minimum loss of 0.28 dB km^{-1} at 1.55 μm. A similar fibre prepared with a commercial silica tube (not depressed index) showed a minimum loss of 3 dB km^{-1} at 0.95 μm, with greatly increased loss at longer wavelengths.

6.2.2. Sintering of porous preforms

Several workers [21–23, 191–193] have examined the sintering step in optical fibre preforms prepared by the three methods. Walker *et al.* [191] studied sequential positions along an MCVD tube. A sample was prepared by simultaneously turning off the torch and reagent flow during the middle of the torch's travel under normal MCVD conditions. The reagents ($SiCl_4$, $GeCl_4$, BCl_3) were delivered by a flow of oxygen of 1100 to 3002 cm^3 min^{-1}, with or without helium admixed (500 cm^3 min^{-1}).

Some electron micrographs of the layers at different temperatures are presented in Fig. 31. As seen, the initial stages of consolidation proceeded via neck formation and growth, then smooth bridges formed and grew more slowly to form a pore-free glass. It was shown that the presence of helium increased the consolidation rate, but no qualitative effect of it on the sintering was observed. The closed pores were irregular in shape, indicating that diffusion of gas out of the closed pores was faster than the transport of glass during pore shrinkage. In the next experiment a very low density layer was deposited on the top of a very dense thin layer. In this case the layer next to the gas stream happened to be SiO_2- poor, and thus of lower viscosity; it therefore sintered more rapidly than the SiO_2-rich layer next to the tube wall. This resulted in the entrapment of a layer of pores beneath 10 μm of the pore-free glass. With further heating these pores continued to shrink and disappear (Fig. 32), confirming that diffusion of gas through the glass is faster than the flow of glass.

Consolidation of these GeO_2–B_2O_3–SiO_2

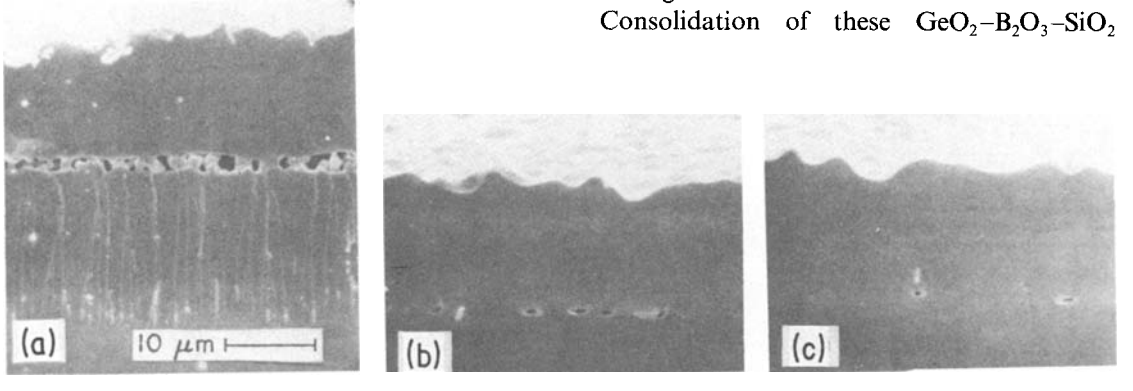

Figure 32 Micrographs (edge views), illustrating that diffusion of gas is faster than mass transport of glass: (a) 1 sec, 900° C; (b) 2 sec, 1600° C; (c) 3 sec, 1600° C (after Walker *et al.* [191]).

layers proceeded both axially (due to progressive heat treatment) and radially (due to a composition gradient). The composition next to the wall had the highest content of GeO_2 and hence the lowest viscosity. Consolidation of pure silica layers proceeded uniformly across the layer due to the lack of a composition gradient [191]. The theory of sintering of MCVD layers based on Frenkel's theory [10] (see Section 2) was developed by Walker *et al.* [191] and showed good agreement with experiment. The consolidation rate was experimentally and theoretically shown to be extremely sensitive to thermal conductivity of the gas and concentration of dopants, the latter through its effect on the viscosity of the material being sintered.

It was shown [191] that bubble formation can occur during collapse of the MCVD preform as a result of incomplete consolidation or excessive deposition temperature. Walker *et al.* [191] established that a critical temperature exists which determines whether the gas flux is in or out of a pore. Above this temperature the closed pore will become a growing bubble. This temperature is determined by equilibrium in the reaction $GeO_2 \rightleftharpoons GeO(g) + \frac{1}{2} O_2(g)$; GeO gas is assumed to fill the growing bubbles. Such bubble growth can be avoided as long as the proper time–temperature programme is chosen, showing that there is no fundamental limit to the thickness of an MCVD layer which can be successfully sintered.

Yan *et al.* [192] studied the sintering of soot similar to that of OVPO boules. It was shown that the microstructure of porous material is similar to that of MCVD. The soot consisted of SiO_2 and B_2O_3 particles, prepared by flame hydrolysis of $SiCl_4$ and BCl_3. This soot was deposited on an aluminium mandrel 1.74 cm in diameter; the oxide layer was about 30 cm long and 0.5 cm thick. This is a significantly higher thickness than layers sintered in the MCVD process. The composition of the layer included 6 wt % B_2O_3. The oxide shell removed from the mandrel was sintered in a flow of helium. Each specimen was preheated to 800° C for 10 min, and then moved into the hot zone for sintering.

The sintering kinetics of the porous material is shown in Fig. 33. The sintering is negligible below 1000° C, then the rate rapidly increases with temperature. The sintering data are described well by the theoretical models of Frenkel [10], Mackenzie and Shuttleworth [11] and Scherer [21–23] exemplified by Figs. 3 and 5. This model (see Equation 4 in Section 2) allows calculation of the viscosity. Yan *et al.* [192], performing such a calculation, found that the values were consistent with the published viscosity data for the borosilicate system. For the glass under study, with 6 wt % B_2O_3, dependence of the viscosity on temperature had the Arrhenius form and could be expressed as η (N sec m^{-2}) = 1.49 exp [215 (kJ)/RT]. Yan *et al.* [192] predicted the necessary temperature adjustment required to maintain the same sintering conditions when the B_2O_3 content is changed. It was shown that increasing the B_2O_3 content reduces the bubble formation phenomenon. The authors [192] maintain that their predictions should be valid for the MCVD process as well. Scherer and Bachman [21–23] also studied the sintering of OVPO preforms (these papers are reviewed in Section 2).

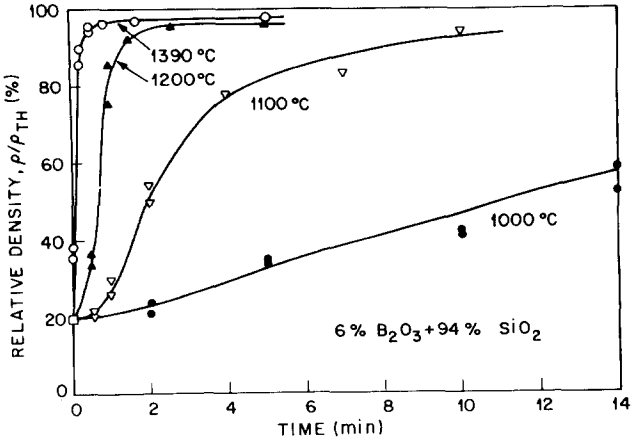

Figure 33 Sintering kinetics of B_2O_3-doped silica glass (after Yan *et al.* [192]).

Sintering in the VAD process was studied by Sudo *et al.* [193]. The significant differences from the MCVD process are: (a) in VAD the sintering at 1500 to 1600° C is not followed by a collapse step at higher temperatures; (b) the atmosphere during sintering can be separated from the atmosphere during deposition and thus can contain pure helium without oxygen; (c) the thickness of a sintered material is much larger. Sudo *et al.* [193] studied the sintering of a cylindrical porous preform 6 cm in diameter and 27 cm in length with a bulk density of 0.3 g cm^{-3}. After sintering the diameter was reduced to 2.5 cm. The preform was prepared by flame hydrolysis of $SiCl_4$, $GeCl_4$ and $POCl_3$. The temperature gradient at the hot zone region was 140° C cm^{-1}, and the pulling speed through the furnace was 0.4 cm min^{-1}†.

Fig. 34 shows the process of sintering in a helium atmosphere; the scheme illustrates the positions in the preform from which the specimens for the micrographs were taken. A progressive sintering to a transparent glass is shown. In contrast, sintering in argon resulted in pore expansion after a closed-spherical pore state was reached, similar to that in Fig. 34d.

Sudo *et al.* [193] developed a theory describing the final stage of sintering and bubble formation. While Walker *et al.* [191] considered the critical temperature for bubble growing in the conditions of changing temperature of the MCVD process (collapse after sintering), Sudo *et al.* [193] were concerned with the critical pore diameter for constant sintering temperatures. The critical diameter d_c determines whether the pore will shrink ($d < d_c$) or expand ($d > d_c$) with temperature increase. The theory for calculation of d_c was developed. For a temperature of 1600 K,

$$d_c = -0.545 \times 10^{-3} + (0.297 \times 10^{-6} + 2.09 \times 10^{2}\, K/CL)^{1/2} \quad (8)$$

where $K = DS$ is the gas permeability in glass, D is the diffusion coefficient of the gas in the glass, S is the solubility of the gas in the glass, $C = \Delta T/\Delta t$ is the rate of temperature increase and L is the glass wall thickness. From operating conditions $C = 1\,\mathrm{K\,sec^{-1}}$, L is estimated as 0.1 cm, K(He) = 8.32×10^{-7} and K(Ar) = 2.27×10^{-11} cm^3 cm^{-1} sec^{-1} atm^{-1} K^{-1}. From these values d_c(He) = 500 μm, while d_c(Ar) = = 0.6 μm. This clearly favours the use of a helium atmosphere for sintering, although bubble-free preform could be produced in argon as well when lower values of C were used. The analysis for mixed gas atmospheres given by Sudo *et al.* [193] is important for dehydration of the VAD preforms in the presence of $SOCl_2$ [194]. Oxygen, bubbled through liquid $SOCl_2$ and saturated with it, was introduced to the consolidation furnace together with helium gas. The final OH content was below 0.5 ppm, and the fibre produced from this preform showed a loss of 0.62 dB km^{-1} at 1.61 μm.

As seen, all three main processes for optical fibre preparation have a lot in common: all require dehydration by Cl_2 or chlorine-containing compounds; all obey Frenkel's theory for the initial stages of sintering; and all require control of the sintering atmosphere and conditions to achieve a bubble-free glass. As discussed, these results were utilized by workers [153, 157] who consolidated gel-derived porous structures to a transparent glass.

Optical fibre science and manufacture represent the highest achievements in glass science and technology, where such parameters as optical attenuation and strength are close to theoretical values. Steady progress in fibre performance and process improvements have resulted in large-scale manufacture at low cost. These achievements have resulted in lightwave communication systems, using glass fibre lightguides as the transmission media, being rapidly implemented in the United States and throughout the world.

7. Summary

In traditional glass-making, melting procedures were inseparable from glass formation. The purpose of this review was to demonstrate that in today's technology sintering techniques are increasingly being used in glass manufacture. These techniques comprise traditional ceramic methods applied mainly to premelted glass powders. However, entirely new methods of glass preparation have also emerged which are unlike any previously known: sol–gel methods, and

† This value is given erroneously by Sudo *et al.* [193] as 4 cm min^{-1}; the correct value has been communicated to the present author by Dr S. Sudo.

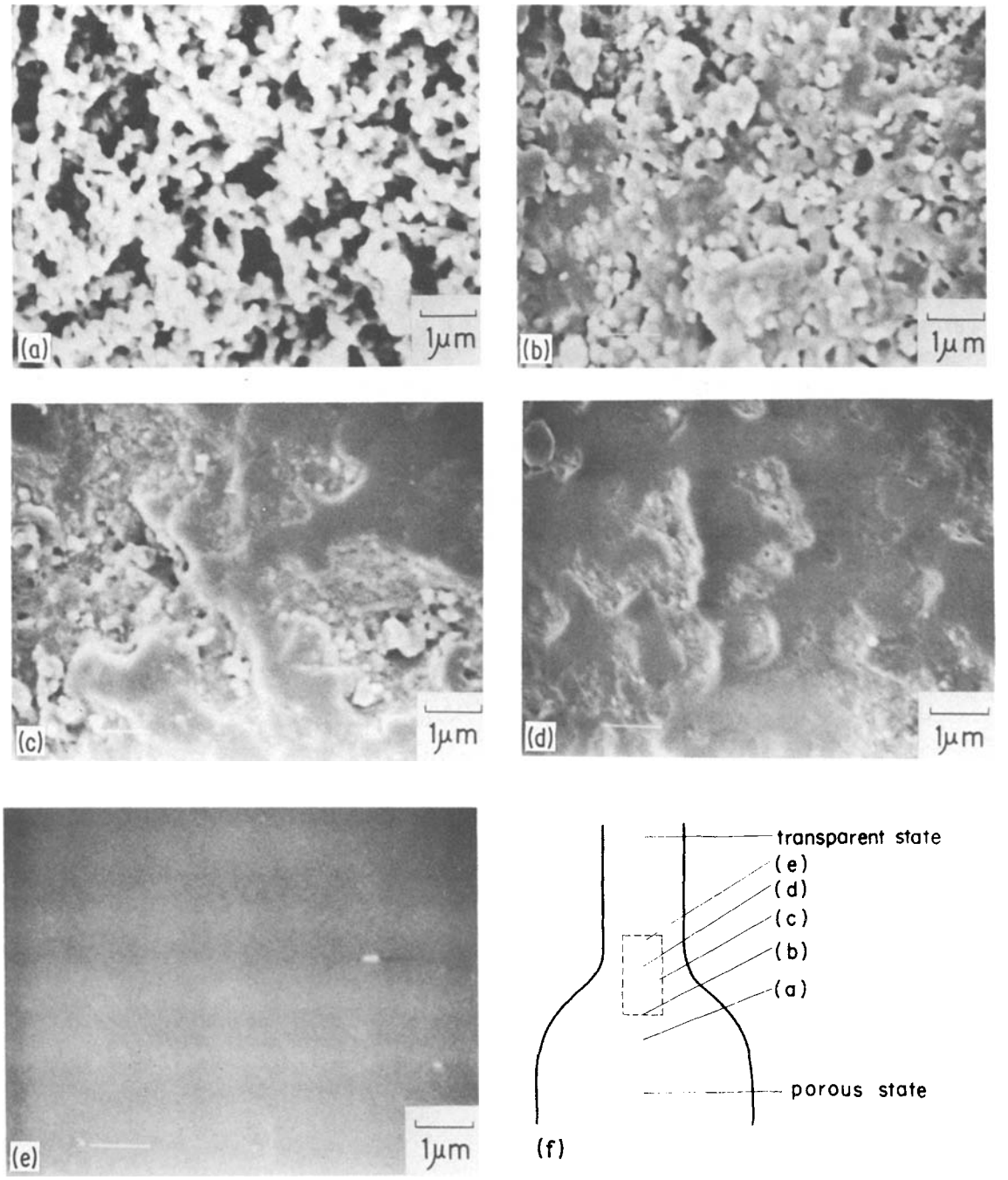

Figure 34 Sintering of a VAD preform in helium: (a) initial pore state; (b) open pore state; (c) closed pore state; (d) closed-spherical pore state; (e) bubble-free transparent glass. The diagram (f) illustrates positions in the preform corresponding to pictures (a) to (e); a dashed line shows the specimen dimensions (the lower diameter of the preform is 6 cm. After Sudo *et al.* [193].

chemical vapour oxidation and hydrolysis deposition. The sol–gel route of glass and ceramic preparation is blossoming as a science but is still in its infancy as technology. In contrast, optical fibre fabrication is a well-established technology which has been developed, and in some aspects perfected, as never before relative to other branches of glass technology. All this may require the rewriting of glass technology textbooks with stronger emphasis on sintering

processes as equal partners with glass melting processes.

Acknowledgements

The author is thankful to M. L. Green, C. R. Kurkjian, J. B. MacChesney, M. J. Matthewson, S. R. Nagel, K. Nassau, and D. L. Wood for reading various parts of the manuscript and for their valuable comments. He is grateful to the authors of the cited papers and to the following publishers for permission to reproduce figures from their publications: The institute of Physics, UK (Fig. 3), John Wiley and Sons, Inc. (Figs. 4, 29), the American Ceramic Society (Figs. 5, 6, 11–14, 17–20, 23–27, 31, 32). Dr. Sh. Sōmiya, editor (Figs. 7, 8), Putnam Publishing Group (Fig. 9), *Physica Scripta* (Fig. 21), North-Holland Physics Publishing (Figs. 22, 28), Ashlee Publishing Co, Inc. (Fig. 30a), Academic Press (Figs. 30b and c), Chapman and Hall Ltd (Fig. 33). Special thanks are due to Dr T. H. Elmer of Corning Glass Works and to Dr S. Sudo of Ibaraki Electrical Communications Laboratory who sent original photographs for Figs. 18 and 34.

References

1. G. W. McLELLAN and E. B. SHAND, "Glass Engineering Handbook" (McGraw Hill, New York, 1984).
2. E. M. LEVIN, C. R. ROBBINS and H. F. McMURDIE, "Phase Diagram for Ceramists" (American Ceramic Society, 1964).
3. D. M. FIELD "Great Masterpieces of World Art" (Crescent, 1979) p. 28.
4. A. D. PEARSON, J. B. MacCHESNEY and W. G. FRENCH, in "Kirk-Othmer Encyclopedia of Chemical Technology", 3rd edition, Vol. 10 (Wiley, 1980) p. 125.
5. P. C. SCHULTZ, *Glass Ind.*, No. 2 (1982) 20.
6. *Idem, ibid.* No. 3 (1982) 26.
7. S. SAKKA, "Treatise on Materials Science and Technology", Vol. 22, Glass III, edited by M. Tomozawa and R. H. Doremus (Academic Press, New York, 1982) p. 129.
8. Proceedings of International Workshop on Glasses and Glass Ceramics from Gels, edited by V. Gottardi, *J. Non-Cryst. Solids* **48** (1) (1982) 1.
9. Proceedings of 2nd International Workshop on Glasses and Glass Ceramics from Gels, edited by H. Scholze, *ibid.* **63** (1/2) (1984) 1.
10. Ya. I. FRENKEL, *J. Phys. USSR* **9** (1945) 385 (in Russian).
11. J. K. MACKENZIE and R. SHUTTLEWORTH, *Proc. Phys. Soc. (Lond.)* **B62** (1949) 833.
12. G. C. KUCZYNSKI, *J. Appl. Phys.* **20** (1949) 1160.
13. G. C. KUCZYNSKI and I. ZAPLATYNSKYJ, *J. Amer. Ceram. Soc.* **39** (1956) 349.
14. I. B. CUTLER and R. E. HENRICKSEN, *ibid.* **51** (1968) 604.
15. I. B. CUTLER, *ibid.* **52** (1969) 14.
16. *Idem, Phys. of Sintering, Ser. 1* **1** (1969) D1.
17. W. D. KINGERY and M. BERG, *J. Appl. Phys.*, **26** (1955) 1205.
18. W. D. KINGERY, H. K. BOWEN and D. R. UHLMANN, "Introduction to Ceramics," 2nd edn. (Wiley, New York, 1976).
19. Ya. E. GEGUZIN, "Fisika Spekaniya" (Physics of Sintering) (Nauka, Moscow, 1967).
20. G. PETZOW, W. A. KAYSSER and M. AMTENBRINK, "Materials Science Monographs 14, Sintering-Theory and Practice," edited by D. Kolar, S. Pejovnik and M. M. Ristić (Elsevier, Amsterdam, Oxford, New York, 1982) p. 27.
21. G. W. SCHERER, *J. Amer. Ceram. Soc.* **60** (1977) (1977) 236.
22. G. W. SCHERER and D. L. BACHMAN, *ibid.* **60** (1977) 239.
23. G. W. SCHERER, *ibid.* **60** (1977) 243.
24. *Idem, J. Non-Cryst. Solids* **34** (1979) 239.
25. T. SHIMOHIRA, A. MAKISHIMA, K. KOTANI and M. WAKAKUWA, in Proceedings of the International Symposium on Factors in Densification and Sintering of Oxide and Non-Oxide Ceramics, Hakone, Japan, October 1978, edited by S. Sōmiya and S. Saito, (Gakujutsu Bunken Fukyu-Kai, Association for Science Documents Information, c/o Tokyo Institute of Technology, Tokyo) p. 119.
26. C. W. PARMELEE, "Ceramic Glazes", 3rd Edn. (Cahners, Chicago, 1973).
27. A. PETZOLD, "Email" (Vel Verlag Technik, Berlin, 1955).
28. A. A. APPEN, "Temperaturoustoichivye Neorganicheskie Pokrytiya" (Temperature-Resistant Inorganic Coatings), 2nd Edn. (Khimiya, Leningrad, 1976).
29. "Neorganicheskie and Organosilikatnye Pokrytiya" (Inorganic and Organosilicate Coatings), Leningrad, March 1973, edited by M. M. Schults (Nauka, Leningrad, 1975).
30. I. I. KITAIGORODSKII (ed.), "Tekhnologiya Stekla" (Glass Technology), 3rd Edn. (Stroilizdat, Moscow, 1961).
31. *Idem, Dokl. Akad. Nauk SSSR* **42** (9) (1944) 407.
32. I. I. KITAIGORODSKII and N. V. SOLOMIN, *ibid.* **56** (6) (1947) 611.
33. M. B. VOLF, "Technical Glasses" (Pitman, London and Prague, 1961).
34. B. ROUS, "Sklo v Elektronike" (Glass in Electronics) (Praha, Státní Nakłada-telství Technické Literatury, 1966).
35. C. H. GREENE, US Patent 2 314 824 (1943).
36. B. V. JANAKIRAMA RAO, *J. Sci. Ind. Res. (India)* **3** (9) (1945) 418.
37. F. SKAUPY and G. WEISSENBERG, US Patent 2 270 718 (1942).
38. *Idem, Ceram. Abstr.* **21** (1942) 80.
39. T. VASILOS, *J. Amer. Ceram. Soc.* **43** (1960) 517.

40. J. D. FLEMING, *Amer. Ceram. Soc. Bull.* **40** (1961) 748.
41. W. SCHULLE and J. ULBRICHT, *Silikattechnick,* **13** (1962) 229.
42. P. P. BUDNIKOV and Yu. E. PIVINSKII, *Russ. Chem. Rev. (English translation of Uspekhi Khimii)* **36** (1967) 210.
43. Yu. E. PIVINSKII and F. T. GOROBETZ, *Glass and Ceramics* (English translation) No. 5 (1968) 285.
44. R. Ya. POPILSKII, L. E. ADUSHKIN, Yu. E. PIVINSKII and F. Ya. BORODAI, *Refractories* (English translation) **12** (1971) 253.
45. D. TAYLOR, A. N. PENNY, A. M. ROBINSON and R. J. A. SMITH, *Proc. Brit. Ceram. Soc.* **22** (1973) 55.
46. Yu. E. PIVINSKII and A. G. ROMASHIN, "Kvartsevaya Keramika" (Quartz Ceramics) (Moscow, 1974).
47. G. M. TOMILOV, N. V. SOLOMIN and T. V. SMIRNOVA, *Inorganic Materials* (English translation) **14** (1978) 145.
48. D. B. MIN'KOV, V. V. KOLOMEITZEV, B. V. PARKHAEV, A. M. TIKHONOVA, N. S. LOGACHEVA, and V. I. GROMOV, *Refractories* (English translation), **20** (1979) 525.
49. R. K. SAVITSKAS and I. S. MATUSEVICH, *Glass and Ceram.* (English translation) **4** (1980) 194.
50. L. A. KOMAROVA, *ibid.* **6** (1980) 305.
51. O. V. MAZURIN, M. V. STRELTSINA, and T. P. SHVAIKO-SHVAIKOVSKAYA, "Physical Sciences Data, Vol. 15: Handbook of Glass Data, Part A: Silica Glass and Binary Silicate Glasses" (Elsevier, Amsterdam, Oxford, New York, Tokyo, 1984).
52. R. E. GANNON, G. M. HARRIS and T. VASILOS, *Amer. Ceram. Soc. Bull.* **44** (1965) 460.
53. J. D. FLEMING, *ibid.* **41** (1962) 472.
54. E. B. JOY, G. K. HUDDLESTON, H. L. BASSETT, C. W. GORTON and S. H. BOMAR Jr, "Analysis and Evaluation of Radome Materials and Configurations for Advanced RF Seekers", Final Report on Projects E-21-628 and A-1535 (Georgia Institute of Technology, 1974).
55. P. W. McMILLAN, "Glass-Ceramics," 2nd Edn (Academic Press, New York, 1979).
56. "Advances in Ceramics", Vol. 4: Nucleation and Crystallization in Glasses, edited by J. H. Simmons, D. R. Uhlmann and G. H. Beall (American Ceramic Society, 1982).
57. D. M. MILLER, US Patent 3 926 648 (1975).
58. E. A. TAKHER and Z. D. PHILIPOVA, *Elektron. Teknika* (in Russian) Ser. 10(9) (1966) 203.
59. E. A. TAKHER, R. Ya. POPILSKII, E. P. DAIN, M. G. LUKOPEROVA and N. A. KIR'YANOVA, *Glass and Ceramics* (English translation) **34** (7) (1977) 445.
60. C. I. HELGESSON, in "Science of Ceramics", Vol. 8 (British Ceramic Society, 1976) p. 347.
61. E. M. RABINOVICH, "Advances in Ceramics", Vol. 4, edited by J. H. Simmons, D. R. Uhlmann and G. H. Beall (American Ceramic Society, Columbus, Ohio, 1982) p. 327.
62. E. A. GIESS, J. P. FLETCHER and L. W. HERRON, *J. Amer. Ceram. Soc.* **67** (1984) 549.
63. P. P. BUDNIKOV, "Technology of Ceramics and Refractories" (MIT Press, Cambridge, Mass., 1964) p. 591.
64. W. SCHILLER and J. WIEGMANN, *Silikattechnik,* **29** (9) (1978) 276.
65. A. E. DALE and J. E. STANWORTH, *J. Soc. Glass Technol.* **33** (1949) 167T.
66. J. BROUKAL, *Silikattechnik* **17** (1966) 242.
67. E. M. RABINOVICH, *Inorganic Mater.* (translated from Russian) **7** (1971) 479.
68. T. TAKAMORI, "Treatise on Materials Science and Technology", Vol. 17, Glass II, edited by M. Tomozawa and R. H. Doremus (Academic, New York, 1979) p. 173.
69. R. H. DALTON, *J. Amer. Ceram. Soc.* **39** (1956) 109.
70. E. M. RABINOVICH, *Amer. Ceram. Soc. Bull.* **58** (1979) 595.
71. A. H. KUMAR and R. R. TUMMALA, *ibid.* **57** (1978) 738.
72. P. W. McMILLAN, B. P. HODGSON and G. PARTRIDGE, British Patent 968 277, cl. ClM (1960).
73. H. P. HOOD and M. E. NORDBERG, US Patent 2 106 744 (1934).
74. T. H. ELMER, *Amer. Ceram. Soc. Bull.* **62** (1983) 513.
75. "The Structure of Glass", Vol. 8, Phase Separation Phenomena in Glasses, edited by E. A. Porai-Koshits, Consultants Bureau, New York, 1972).
76. M. TOMOZAWA, "Treatise on Materials Science and Technology", Vol. 17, Glass II, edited by M. Tomozawa and R. H. Doremus (Academic, New York, 1979) p. 71.
77. R. ROY, *J. Amer. Ceram. Soc.* **43** (1960) 670.
78. I. I. KITAIGORODSKII, E. M. RABINOVICH and V. I. SHELUBSKII, *Glass and Ceramics* (translated from Russian) **20** (1963) 624.
79. W. HALLER, D. H. BLACKBURN, F. E. WAGSTAFF and R. J. CHARLES, *J. Amer. Ceram. Soc.* **53** (1970) 34.
80. T. H. ELMER, M. E. NORDBERG, G. B. CARRIER and E. J. KORDA, *ibid.* **53** (1970) 171.
81. I. I. KITAIGORODSKII, *Dokl. Akcad. Nauk SSSR* **64** (1949) 219.
82. E. M. RABINOVICH, M. ISH-SHALOM and A. KISILEV, *J. Mater. Sci.* **15** (1980) 2027.
83. *Idem, ibid.* **15** (1980) 2039.
84. M. A. RES, J. T. FOURIE and R. W. WHITE, *J. Amer. Ceram. Soc.* **65** (1982) 184.
85. M. A. RES, S. HART and R. W. WHITE, *ibid.* **66** (1983) 221.
86. A. DIETZEL and H. WICKERT, *Glastechn. Ber.* **29** (1) (1956) 1.
87. D. R. UHLMANN, B. J. J. ZELINSKY and G. E. WNEKI, "Better Ceramics Through Chemistry", edited by C. J. Brinker, D. E. Clark and D. R. Ulrich (North-Holland, New York, Amsterdam, Oxford, 1984) p. 59.
88. R. ROY, *J. Amer. Ceram. Soc.* **52** (1969) 344.
89. H. DISLICH, *Angew. Chemie* **10** (1971) 363.
90. C. J. BRINKER, K. D. KEEFER, D. W. SCHAEFER, R. A. ASSINK, B. D. KAY and C. S. ASHLEY, *J. Non-Cryst. Solids* **63** (1984) 45.

91. C. J. BRINKER and G. W. SCHERER, "Ultrastructure Processing of Ceramics, Glasses and Composites", edited by L. L. Hench and D. R. Ulrich (Wiley, New York, 1984) p. 43.
92. C. J. BRINKER and S. P. MUKHERJEE, *J. Mater. Sci.* **16** (1981) 1980.
93. L. C. KLEIN and G. J. GARVEY, *J. Non-Cryst. Solids* **48** (1982) 97.
94. S. SAKKA, and K. KAMIYA in Proceedings of International Symposium on Factors in Densification and Sintering of Oxide and Non-Oxide Ceramics, Hakone, Japan, October 1978, edited by S. Sōmiya and S. Saito, (Gakujutsu Bunken Fukgu-Kai, Association for Science Documents Information, c/o Tokyo Institute of Technology, Tokyo) p. 101.
95. K. KAMIYA, S. SAKKA and Y. TATEMICHI, *J. Mater. Sci.* **15** (1980) 1765.
96. B. E. YOLDAS, *ibid.* **12** (1977) 1203.
97. *Idem, ibid.* **14** (1979) 1845.
98. *Idem, J. Non-Cryst. Solids* **51** (1982) 105.
99. *Idem, ibid.* **63** (1984) 145.
100. J. ZARZYCKI, *ibid.* **48** (1982) 105.
101. S. P. MUKHERJEE, J. ZARZYCKI and J. P. TRAVERSE, *J. Mater. Sci.* **11** (1976) 341.
102. M. DECOTTIGNIES, J. PHALIPPOU and J. ZARZYCKI, *ibid.* **13** (1978) 2605.
103. R. JABRA. J. PHALIPPOU and J. ZARZYCKI, *J. Non-Cryst. Solids* **42** (1980) 489.
104. "Ultrastructure Processing of Ceramics, Glasses and Composites", edited by L. L. Hench nd D. R. Ulrich (Wiley, New York, 1984).
105. "Better Ceramics Through Chemistry" edited by C. J. Brinker, D. E. Clark and D. R. Ulrich (North-Holland, New York, Amsterdam, Oxford, 1984).
106. D. C. BRADLEY, R. C. MEHROTRA and D. P. GAUR, "Methal Alkoxides" (Academic Press, 1978).
107. M. TARASEVICH, Abstract no. 101–G–84 in *Ceramic. Bull.* **63** (1984) 500.
108. R. K. ILER, "The Chemistry of Silica" (Wiley, New York, 1979).
109. L. D. BELYAKOVA, O. M. DZHIGIT, A. V. KISILEV, G. G. MUTTIK and K. D. SHCHERBAKOVA, *Russ. J. Phys. Chem.* (English translation) **33** (1959) 551.
110. D. M. KROL and J. G. van LIEROP, *J. Non-Cryst. Solids* **63** (1984) 131.
111. D. P. PARTLOW and B. E. YOLDAS, *ibid.* **46** (1981) 153.
112. E. M. RABINOVICH, *ibid.* **71** (1985) 187.
113. B. E. WARREN and J. BISCOE, *J. Amer. Ceram. Soc.* **21** (1938) 259.
114. W. W. WARREN Jr, B. GOLDING and E. M. RABINOVICH, *Bull. Amer. Phys. Soc.* **28** (1983) 455.
115. G. GOLDING, W. H. HAEMMERLE, D. L. FOX and E. M. RABINOVICH, *ibid.*
116. W. C. LaCOURSE, M. M. AHKTAR, S. DAHAR, R. D. SANDS and J. STEINMETS, *J. Canad. Ceram. Soc.* **52** (1983) 18.
117. S. HENNING and L. SVENSSON, *Physica Scripta* **23** (1981) 697.
118. M. YAMANE, S. ASO and T. SAKAINO, *J. Mater. Sci.* **13** (1978) 865.
119. M. PRASSAS, J. PHALIPPOU and J. ZARZYCKI, *ibid.* **19** (1984) 1656.
120. M. NOGAMI and Y. MORIYA, *J. Non-Cryst. Solids* **37** (1980) 191.
121. S. L. ANTONOVA and V. V. D'YAKOVA, *Sov. J. Glass Phys. and Chem.* (English translation) **5** (1979) 607.
122. T. WOIGNIER, J. PHALIPPOU and J. ZARZYCKI, *J. Non-Cryst. Solids* **63** (1984) 117.
123. I. M. THOMAS, US Patent 3 767 432 (1973).
124. *Idem,* US Patent 3 767 434 (1973).
125. J. W. FLEMING, private communication (1983).
126. J. SCHLICHTING and S. NEUMANN, *J. Non-Cryst. Solids* **48** (1982) 185.
127. B. E. YOLDAS, "International Congress on Glass XII", Albuquerque, N. Y. 6 to 11 July (1980), edited by R. H. Doremus, W. C. LaCourse, J. D. Mackenzie, J. R. Varner and W. W. Wolf (North-Holland, Amsterdam, New York, Oxford, 1980) p. 81.
128. M. YAMANE, S. INOUE and K. NAKAZAWA, *J. Non-Cryst. Solids* **48** (1982) 153.
129. C. J. R. GONZALES-OLIVER, P. F. JAMES and H. RAWSON, *ibid.* **63** (1984) 129.
130. R. PUYANE, P. F. JAMES and H. RAWSON, *ibid.* **41** (1980) 105.
131. M. PRASSAS, J. PHALIPPOU and L. L. HENCH, *ibid.* **48** (1982) 79.
132. *Idem, ibid.* **63** (1984) 375.
133. T. HAYASHI and H. SAITO, *J. Mater. Sci.* **15** (1980) 1971.
134. M. YAMANE and T. KOJIMA, *J. Non-Cryst. Solids* **44** (1980) 181.
135. M. GUGLIELMI and G. PRINCIPI, *ibid.* **48** (1982) 161.
136. S. P. MUKHERJEE and J. ZARZYCKI, *J. Amer. Ceram. Soc.* **62** (1979) 1.
137. W. HÖLAND, E. R. PLUMAT and P. H. DUVIGNEAUD, *J. Non-Cryst. Solids* **48** (1982) 205.
138. F. PANCRAZI, J. PHALIPPOU, F. SORRENTINO and J. ZARZYCKI, *ibid.* **63** (1984) 81.
139. ZHU CHONGSHEN, HOU LISONG, GAN FUXI and JIANG ZHONJHONG, *ibid.* **63** (1984) 105.
140. S. P. MUKHERJEE, *ibid.* **63** (1984) 35.
141. *Idem, ibid.* **42** (1980) 477.
142. V. GOTTARDI, *ibid.* **49** (1982) 461.
143. M. C. WEINBERG, G. F. NEILSON and G. L. SMITH, *J. Mater. Sci.* in press.
144. J. D. MACKENZIE, *J. Non-Cryst. Solids* **48** (1982) 1.
145. M. C. WEINBERG and G. F. NEILSON, *J. Mater. Sci.* **13** (1978) 1206.
146. *Idem,* "Materials Processing in the Reduced Gravity Environment of Space", edited by G. E. Rindone (Elsevier, Amsterdam, Oxford, New York, Tokyo, 1982) p. 333.
147. *Idem, J. Amer. Ceram. Soc.* **66** (1983) 132.
148. *Idem, J. Non-Cryst. Solids* **63** (1984) 365.
149. R. D. SHOUP, "Colloid and Interface Science", Vol. III, edited by M. Kerker (Academic press, New York, 1976).
150. R. D. SHOUP and W. J. WEIN, US Patent 4 059 658 (1977).
151. E. M. RABINOVICH, D. W. JOHNSON Jr,

J. B. MacCHESNEY and E. M. VOGEL, *J. Non-Cryst. Solids* **47** (1982) 435.
152. *Idem, J. Amer. Ceram. Soc.* **66** (1983) 683.
153. D. W. JOHNSON Jr, E. M. RABINOVICH, J. B. MacCHESNEY and E. M. VOGEL, *ibid.* **66** (1983) 688.
154. D. L. WOOD, E. M. RABINOVICH, J. W. JOHNSON Jr, J. B. MacCHESNEY and E. M. VOGEL, *ibid.* **66** (1983) 693.
155. D. W. JOHNSON Jr, J. B. MacCHESNEY and E. M. RABINOVICH, US Patent 4419115 (1983).
156. E. M. RABINOVICH, J. B. MacCHESNEY, D. W. JOHNSON Jr, J. R. SIMPSON, B. M. MEAGHER, F. V. DiMARCELLO, D. L. WOOD and E. A. SIGETY, *J. Non-Cryst. Solids* **63** (1984) 155 (discussion p. 178).
157. E. M. RABINOVICH, J. B. MacCHESNEY, D. W. JOHNSON Jr, J. W. FLEMING and D. L. CHADWICK, in "The Impact of Energy and Environment on the Science and Technology of Glasses", Abstracts of Annual Meeting of International Commission on Glasses, Toronto, Canada, October (National Research Council of Canada, 1982) p. 8.
158. G. W. SCHERER and J. C. LUONG, *J. Non-Cryst. Solids* **63** (1984) 163 (discussion p. 178).
159. M. D. SACKS and T. -Y. TSENG, *J. Amer. Ceram. Soc.* **67** (1984) 526.
160. *Idem, ibid.* **67** (1984) 532.
161. H. E. MEISSNER and S. D. STOOKEY, US Patent 3827893 (1974).
162. K. S. MAZDIYASNI, "Better Ceramics Through Chemistry", edited by C. J. Brinker, D. E. Clark and D. R. Ulrich (North-Holland, New York, Amsterdam, Oxford, 1984) p. 37.
163. *Research and Development* (April 1984) p. 51.
164. K. SUSA, I. MATSUYAMA, S. SATOH and T. SUGANUMA, *Electronics Lett.* **18** (1982) 499.
165. "Casarett and Doull's Toxicology", 2nd Edn., edited by J. Doull, C. D. Klaassen and M. O. Amdur (Macmillan, New York, 1980) p. 471.
166. A. L. HARMER, R. PUYANE and C. GONZALEZ-OLIVER, *IFOC* (November/December 1982) p. 40.
167. W. C. LaCOURSE, M. M. AKHTAR and S. DAHAR, *J. and Commun. Amer. Ceram. Soc.* **67** (1984) 200.
168. W. C. LaCOURSE, "Better Ceramics Through Chemistry", edited by C. J. Brinker, D. E. Clark and D. R. Ulrich (North-Holland, New York, Amsterdam, Oxford, 1984) p. 53.
169. K. C. KAO and G. A. HOCKMAN, *Proc. IEEE* **113** (1966) 1151.
170. F. P. KAPRONG, D. B. KECK, and R. D. MAURER, *Appl. Phys. Lett.* **17** (1970) 423.
171 J. B. MacCHESNEY, "Preparation and Characterization of Materials", (Academic, New York, 1981) p. 537.
172. "Advances in Ceramics", Vol. 2, Physics of Fiber Optics (American Ceramic Society, Columbus, Ohio, 1981).
173. T. OKOSHI, "Optical Fibers" (Academic, New York, 1982).
174. J. F. HYDE, US Patent 2272342 (1942).
175. J. B. MacCHESNEY and P. B. O'CONNOR, US Patent 4217027 (1980).
176. J. B. MacCHESNEY, P. B. O'CONNOR and H. E. PRESBY, *Proc. IEEE* **62** (1974) 1278.
177. J. B. MacCHESNEY, P. B. O'CONNOR, F. V. DiMARCELLO, J. R. SIMPSON, and P. D. LAZAY, Proceedings of 10th International Congress on Glass, Kyoto, Japan, July 1974, edited by M. Kunugi, M. Tashiro and N. Saga (Ceram. Soc. Japan, 1974) No. 6, p. 6–40.
178. J. R. SIMPSON, J. B. MacCHESNEY and K. L. WALKER, *J. Non-Cryst. Solids* **38/39** (1980) 831.
179. S. R. NAGEL, J. B. MacCHESNEY and K. L. WALKER, *IEEE J. Quantum Electronics* **QE–18** (4) (1982) 459.
180. K. L. WALKER, G. M. HOMSY and F. T. GEYLING, *J. Colloid Interf. Sci.* **69** (1979) 138.
181. J. W. FLEMING and P. B. O'CONNOR, "Preparation and Characterization of Materials" (Academic, New York, 1981) p. 21.
182. K. L. WALKER and R. CSENCSITS, Proceedings of the Topical Meeting on Optical Fiber Communication, OFC '82, Phoenix Arizona, April 1982, 'Post Deadline Papers, Paper PD1.
183. J. W. FLEMING "Technical Digest of Topical Meeting on Optical Fiber Communication", OFC, '83, New Orleans, February/March 1983 (Optical Society of America, 1983) p. 88.
184. T. IZAWA, S. KOBOYASHI, S. SUDO and F. HANAWA, "Technical Digest of International Conference on Integrated Optics, Optical Fiber Communication", (IEEE, Tokyo, Japan, 1977) p. 375.
185. T. IZAWA and N. INAGAKI, *Proc. IEEE* **68** (1980) 1184.
186. R. CSENCSITS, P. J. LEMAIRE, W. A. REED, D. S. SHENK and K. L. WALKER, "Technical Digest of Conference on Optical Fiber Communication", OFC '84, New Orleans, January 1984 (Optical Society of America, 1984) p. 54.
187. V. J. MAZURCZYK, N. S. BERGANO, R. E. WAGNER, K. L. WALKER, N. A. OLSSON, L. G. COHEN, R. A. LOGAN and J. C. CAMPBELL, "Proceedings of 10th European Conference on Optical Fibre Communication", Stuttgart, September 1984, Post Deadline Papers (VDE-Verlag GmBH, 1984) Paper PD–7.
188. K. RAU, A. MÜHLICH and N. TREBER, Proceedings of the Topical Metting on Optical Fiber Transmission II (Williamsburg, Virginia, 1977).
189. T. MIYA, M. NAKAHARA, F. HANAWA and J. OHMORI, Proceedings of the 10th European Conference on Optical Fibre Communication, Stuttgart, September 1984 (VDE-Verlag GmBH, 1984) p. 294.
190. J. B. MacCHESNEY, D. W. JOHNSON Jr, P. J. LEMAIRE, L. G. COHEN and E. M. RABINOVICH, OFC/OFS '85, Conference on Optical Fibre Communication, 11–13 February 1985, and 3rd International Conference on Optical Fibre Sensors, 13–14 February 1985, San Diego, California, Technical Digest (Optical Society of America, San Diego, 1985) pp. 98–100.

191. K. L. WALKER, J. W. HARVEY, F. T. GEYLING and S. R. NAGEL, *J. Amer. Ceram. Soc.* **63** (1980) 96.
192. M. F. YAN, J. B. MacCHESNEY, S. R. NAGEL and W. W. RHODES, *J. Mater. Sci.* **15** (1980) 1371.
193. S. SUDO, T. EDAHIRO and M. KAWACHI, *Trans. IECE Jpn.* **E63** (1980) 731.
194. K. CHIDA, F. HANAWA, M. NAKAHARA and N. INAGAKI, *Electron. Lett.* **15** (1979) 835.

Received 15 November 1984
and accepted 13 March 1985